

**DO NOT DESTROY  
RETURN TO LIBRARY**

NASA CR-135154

DEVELOPMENT OF FAR INFRARED ATTENUATION TO  
MEASURE ELECTRON DENSITIES IN CW PIN  
DISCHARGE LASERS

R. V. Babcock  
Westinghouse R&D Center  
Pittsburgh, Pennsylvania 15235

Prepared for

National Aeronautics and Space Administration

Contract NAS3-19702

NASA-CR-135154

28 JUN 1977  
MCDONNELL DOUGLAS  
RESEARCH & ENGINEERING LIBRARY  
ST. LOUIS

M77-14231

1 Report No CR-135154		2 Government Accession No		3 Recipient's Catalog No	
4 Title and Subtitle Development of Far Infrared Attenuation to Measure Electron Densities in CW Pin Discharge Lasers				5 Report Date	
7 Author(s) R. V Babcock				6 Performing Organization Code	
9 Performing Organization Name and Address Westinghouse Research Laboratories Pittsburgh, PA 15235				8 Performing Organization Report No	
12 Sponsoring Agency Name and Address National Aeronautics and Space Administration Washington, DC 20546				10 Work Unit No R6863	
				11 Contract or Grant No NAS3-19702	
				13 Type of Report and Period Covered Final Report	
15 Supplementary Notes Project Manager, Eugene J. Manista, Laser Engineering Section, NASA Lewis Research Center, Cleveland, Ohio				14 Sponsoring Agency Code 6344	
16 Abstract A two beam attenuation technique was devised to measure electron densities of $10^9 - 10^{11} \text{ cm}^{-3}$ , resolved to 1 cm, in a near-atmospheric COFFEE laser discharge, using 496 $\mu\text{m}$ and 1220 $\mu\text{m}$ radiations from $\text{CH}_3\text{F}$ , optically pumped by a $\text{CO}_2$ laser. A far infrared generator was developed which was suitable except for a periodic intensity variation in FIR output deriving from frequency variation of the pump radiation. Because the available pump laser could not be stabilized in output frequencies to the required $\pm 2$ MHz, the planned electron density studies were not conducted.					
17 Key Words (Suggested by Author(s)) lasers fusion glow discharges ultraviolet carbon dioxide			18 Distribution Statement COFFEE attenuation electron density Unclassified - Unlimited		
19 Security Classif (of this report) Unclassified		20 Security Classif (of this page) Unclassified		21 No of Pages	22 Price*

\* For sale by the National Technical Information Service, Springfield, Virginia 22161

DEVELOPMENT OF FAR INFRARED ATTENUATION TO MEASURE  
ELECTRON DENSITIES IN CW PIN DISCHARGE LASERS

R. V. Babcock  
Westinghouse R&D Center  
Pittsburgh, Pennsylvania 15235

ABSTRACT

A two beam attenuation technique was devised to measure electron densities of  $10^9 - 10^{11} \text{ cm}^{-3}$ , resolved to 1 cm, in a near-atmospheric COFFEE laser discharge, using 496  $\mu\text{m}$  and 1220  $\mu\text{m}$  radiations from  $\text{CH}_3\text{F}$ , optically pumped by a  $\text{CO}_2$  laser. A far infrared generator was developed which was suitably except for a periodic intensity variation in FIR output deriving from frequency variation of the pump radiation. Because the available pump laser could not be stabilized in output frequencies to the required  $\pm 2$  MHz, the planned electron density studies were not conducted.

DEVELOPMENT OF FAR INFRARED ATTENUATION TO MEASURE  
ELECTRON DENSITIES IN CW PIN DISCHARGE LASERS

R. V. Babcock  
Westinghouse R&D Center  
Pittsburgh, Pennsylvania 15235

1. SUMMARY

The contract goals were to develop a two frequency, FIR attenuation technique capable of measuring electron densities (in typical COFFEE laser gas mixtures having high collision frequencies) to 1 cm spatial resolution in the two dimensions transverse to the optic axis of the Westinghouse cw COFFEE laser, to conduct parametric studies of electron density in the 10 cm cubical COFFEE discharge module at the Westinghouse CRL, and to apply the technique to the High Power Laser Test Facility at the NASA Lewis Research Center. The physical constraints corresponding to these goals dictated the use of two FIR probe beams of sufficiently different wavelengths, within the approximate range of wavelengths 500  $\mu\text{m}$  - 1000  $\mu\text{m}$ , which could be generated cw with adequate intensity and beam quality to permit measurement of attenuation to 1 part in  $10^4$ . Two transitions in  $\text{CH}_3\text{F}$  were selected, at 496  $\mu\text{m}$  and 1220  $\mu\text{m}$ , which are optically excited by the P(20) and P(32) lines, respectively, of the 9.5  $\mu\text{m}$  band from a line selectable  $\text{CO}_2$  pump laser. Attenuation was to be measured to the necessary precision by chopping the FIR beam alternatively into carefully matched test and reference paths, combining the beam at the detector, and measuring the difference signal with a lock-in amplifier system. This procedure called for a stable cw FIR source emitting a few mW with a beam divergence <100 milliradians.

An open cavity, hole-coupled FIR generator was developed which emitted 0.5 mW at 496  $\mu\text{m}$ , but had marginal gain, requiring an output aperture  $\leq 4$  mm in diameter. Diffraction from such an aperture implied excessive beam divergence. We decided that a hole-coupled generator would not suffice.

A dielectric waveguide cavity FIR generator was built having a 25 mm aperture, partially transmitting output. This configuration emitted 1.6 mW at 496  $\mu\text{m}$ , with satisfactory beam divergence. It would suffice if the cavity length of the  $\text{CO}_2$  pump laser could be stabilized so that the frequency of the P(20) line could be held constant to a few mHz. This stabilization, achieved by active piezoelectric length tuning, had been successfully demonstrated in a very similar application elsewhere.

With the contract termination date approaching, we found that the inherent stability of our pump laser was so poor that we were unable to stabilize the  $\text{CO}_2$  output frequency during the contracted period. Accordingly, after consultation with the contract monitor, the contract was terminated on schedule, with some contract goals unfulfilled.

## 2. INTRODUCTION

### 2.1 Contract Goals and Approach

The goals of this contract were

1. To develop a technique for measuring electron density in the presence of high collision frequencies within the active discharge volume of the Westinghouse cw COFFEE laser, capable of providing electron density values spatially resolved to 1 cm or better in the two dimensions transverse to the optic axis, and averaged over the 10 cm path length along the optic axis, in the existing Westinghouse 10 x 10 x 10 cm COFFEE discharge test module.
2. To apply the technique to parametric studies of the behavior of the COFFEE discharge, in the test module. The behavior of the COFFEE discharge is not completely understood, and this is impeding the full development of this very promising cw CO<sub>2</sub> laser technology.
3. To adapt the technique to study electron density distributions in the 1.5 meter High Power Laser Test facility at the NASA Lewis Research Center.

In the fully developed, flow stabilized DC discharge of the COFFEE laser, electron densities are roughly  $3 \times 10^{10} \text{ cm}^{-3}$ . In order to observe the growth and decay of these electron densities, one desires a measurement technique that is sensitive to the order of  $10^9$  electrons/cm<sup>3</sup>. To measure this range of electron densities in the presence of 0.5 - 1 atm of neutral gas molecules is difficult. After examining the possible techniques, we chose to measure the single-pass attenuation of a diffraction limited beam of electromagnetic radiation.

This method had previously been employed with considerable success at the Westinghouse Research Laboratories<sup>1</sup> to measure electron densities in the range  $10^{12} - 10^{13} \text{ cm}^{-3}$ , encountered in our pulsed  $\text{CO}_2$  lasers, which are pumped by self-sustained electric discharges. In Fig. 1, electron densities measured by the two-pass attenuation of a  $337 \text{ }\mu\text{m}$  beam of far infrared (FIR) radiation are compared with values calculated from the electron drift velocity corresponding to the known value of  $E/N$  in the discharge. The agreement is excellent.  $E/N$  is the ratio of electric field strength to neutral gas density. In the pulsed laser discharge,  $E/N$  is well understood, and we can reliably calculate  $E/N$  from the applied voltage and the gas conditions, and thus calculate electron drift velocity and electron number density ( $n_e$ ). In the COFFEE discharge, however, we do not have adequate models to describe the behavior of  $E/N$ , and cannot reliably calculate  $n_e$  from the observed discharge parameters.

The above measurements used a beam of  $337 \text{ }\mu\text{m}$  radiation from an HCN laser, operating cw, which passed twice through the discharge volume, and was detected by an InSb detector cooled to  $4^\circ\text{K}$ . When the discharge was pulsed on, attenuation of 1% or more resulting from the appearance of free electrons could be discerned. Although this sensitivity was adequate for the above purpose, the range of  $n_e$  expected in the COFFEE discharge provides much less than the 1% attenuation which we could discern in a pulsed measurement. To obtain the needed sensitivity, one must measure the electronic attenuation to one part in  $10^4$ . This we proposed to do with the chopped dual beam measurement sketched in principle in Fig. 2. First, with no discharge, the test and reference beams are equalized by a variable external attenuation until the difference signal from a phase-sensitive amplifier locked to the chopping frequency is nulled. Then the discharge is established, and the difference signal measures the electronic attenuation of the test beam. It was also necessary to choose two probing wavelengths, both lying in a different wavelength range from the  $337 \text{ }\mu\text{m}$  used above. Two different wavelengths are needed to separately determine  $n_e$  and  $\nu$ , the collision frequency, as discussed below.

## 2.2 Choice of Probe Wavelengths

The applicable range of FIR wavelengths is limited from above by the requirement of 1 cm transverse spatial resolution over a 10 cm path length, and from below by the need for high sensitivity, due to the relatively low electron densities encountered in the COFFEE discharge. Assuming diffraction limited beam divergence the longest wavelength radiation which can be contained\* within a tube 1 cm in diameter by 10 cm long is about 1000  $\mu\text{m}$ --this determined the upper limit. The lower bound derives from the relation governing electromagnetic wave propagation through a weakly ionized, collision dominated plasma, which reduces, for our particular conditions\*\*, to

$$\alpha = 0.1059 \nu n_e / (\nu^2 + \omega^2), \quad (1)$$

where  $\alpha$  is the attenuation constant per cm,  $\nu$  is the collision frequency for momentum transfer, and  $\omega$  is the radian frequency of the wave. For the required sensitivity of  $\alpha$  times 10 cm  $\geq 10^{-4}$  at an electron density of  $n_e = 10^9 \text{ cm}^{-3}$ , given the approximately known values of  $\nu$  for the COFFEE neutral gas conditions, Eq. (1) requires that  $\omega$  correspond to a wavelength  $\gtrsim 500 \mu\text{m}$ .

Within this wavelength range, the two most suitable sources were chosen as the 496  $\mu\text{m}$  and 1220  $\mu\text{m}$  emissions from  $\text{CH}_3\text{F}$ . Taking calculated values of  $\nu$  for typical COFFEE laser gas compositions, we show in Table 1 the values of minimum detectable electron density

---

\* A simplified calculation using relations valid in the far field goes as follows: A lens of diameter  $d$  and focal length  $f$  is positioned to focus the FIR beam at the center of the tube. By geometric optics we require  $f/d \geq 5$  for the beam diameter not to exceed 1 cm at the entrance to the tube. Since the diffraction half angle is  $\theta = 1.2 \lambda/d$  radians, the diameter of the focal spot will be  $D = 2f\theta = 2.4 \lambda f/d$ . Therefore  $D \geq 12\lambda$ , and  $D = 1 \text{ cm}$  implies  $\lambda \leq 833 \mu\text{m}$ . The actual case of a Gaussian beam in the near field is more complicated, and the criterion given in the text is only a rough approximation.

\*\* i.e., plasma frequency  $\ll \nu^2 + \omega^2$ .



corresponding to an attenuation of one part in  $10^4$  over 10 cm, for these two probe wavelengths. Since we assume that an attenuation of  $10^{-4}$  can be observed with a signal to noise ratio of 1, the minimum detectable electron density is also the uncertainty in the measured value of  $n_e$ , when  $\nu$  is known independently. Thus if  $n_e \sim 3 \times 10^{10}$ , it should be possible to determine relative values of  $n_e$  (i.e., assuming  $\nu$  is independent of position) to a precision of 2 to 5%, depending on gas composition and pressure, by measuring the single pass attenuation of 1220  $\mu\text{m}$  radiation ( $\omega_1 = 1.5 \times 10^{12} \text{ sec}^{-1}$ ). For example, if  $n_e$  is measured in a 1:7:20 mixture at 450 Torr, at the two positions A and B, then each measurement has a precision of  $3.04 \times 10^8 / 3 \times 10^{10} = 1\%$ . Then  $n_e$  at A is known, relative to  $n_e$  at B, to a precision of 2%.

To obtain an absolute value of  $n_e$  with a useful degree of accuracy is far more difficult. One must separately determine  $\nu$  and  $n_e$  by measuring the attenuation at two sufficiently distinct FIR frequencies,  $\omega_1$  and  $\omega_2$ . Then Eq. (1) can be applied twice to give the ratio

$$\rho \equiv (\alpha_1/\alpha_2) = (\nu^2 + \omega_2^2)/(\nu^2 + \omega_1^2), \quad (2)$$

which depends only on  $\nu$  and the known probe frequencies. This dependence is shown in Fig. 3. Clearly, if we wish to determine  $\nu$  with any precision, we must choose  $\omega$  in the vicinity of  $\nu$ , where  $\rho$  is changing most rapidly. This strategy becomes even more necessary when we consider the sensitivity of Eq. (1) to the error in determining  $\nu$ . Taking the partial differential of Eq. (1) with respect to  $\nu$ , the fractional error in  $n_e$  is seen to depend on the fractional error in  $\nu$  as

$$(\Delta n_e/n_e) = (\Delta \nu/\nu) (\omega^2 - \nu^2)/(\omega^2 + \nu^2). \quad (3)$$

One notes that when  $\omega \sim \nu$ , the measurement of  $n_e$  will be relatively immune from error due to the uncertainty in the measured value of  $\nu$ .

To examine the combined effect, one eliminates  $\nu$  between Eqs. (1) and (2) to give explicitly  $\Delta n_e$ , the uncertainty in  $n_e$  which results from measuring  $\alpha_1$  and  $\alpha_2$  with signal to noise ratios of  $10^4$ ,

$$\Delta n_e = \frac{9.45\omega_1(r^2-1)}{[(\rho-1)(r^2-\rho)]^{1/2}} \{ \Delta\alpha_1 + \frac{\rho|r^{2-2\rho+1}|}{2(\rho-1)(r^2-\rho)} (\rho\Delta\alpha_2 + j\Delta\alpha_1) \}, \quad (4)$$

where  $r \equiv \omega_2/\omega_1 = 2.5$ ,  $j = 1$ , and  $\Delta\alpha_1 = \Delta\alpha_2 = 10^{-5}$ , corresponding to a measurement uncertainty of  $\Delta(L\alpha) = 10^{-4}$  over a path length of  $L = 10$  cm. Equation (4) is given by the solid curve in Fig. 4. The two bars at lower left indicate the calculated ranges of  $\nu$  for the two typical COFFEE laser gas mixtures, as given in Table 1. The dotted curve obtained by setting  $j = -1$  when  $\nu > \omega_1$ , results from a cancellation of errors which may not be experimentally realistic. The difference is not important, because it occurs only in a region which is not accessible to our measurement.

One sees from Fig. 4 that we made the proper choice of probe frequencies, since  $\omega_1$  is as small as possible consistent with 1 cm spatial resolution (actually, a bit too small). Still, we fall short of the rather sharp requirement that  $\nu \sim \omega_1$ , which seriously degrades the potential accuracy of the absolute measurement of  $n_e$ . The quantitative effect is shown in the column labelled " $\nu$  intrinsic" in Table 1, which gives the uncertainty  $\Delta n_e$  in the absolute measurement of  $n_e$ , if we apply the two frequency method to measure  $\nu$  separately at each gas condition. Strictly, these values of  $\Delta n_e$  apply only when  $n_e \gg \Delta n_e$ . When  $\Delta n_e \sim n_e$ , then  $\Delta n_e$  is  $\sim 3$  times larger. This procedure is clearly inadequate.

A more accurate procedure is to operate each gas composition at the highest pressure and current density which permit a stable discharge, and determine  $\nu$  via Eq. (2). If, as expected,  $\nu$  does not depend significantly on current density or field, these values can be corrected for their linear pressure dependence to obtain a value for  $\nu$  at any discharge condition. The  $n_e$  may be obtained from Eq. (1) by attenuation

measurements at 1220  $\mu\text{m}$ . As an example, if the two gas compositions in Table 1 were measured at 450 Torr and an electron density  $n_e \sim 3 \times 10^{10} \text{ cm}^{-3}$ ,  $\nu$  could be determined with uncertainties of about 15.3% and 11%, respectively. Assuming the same percentage accuracy for the corrected values of  $\nu$ , a 1220  $\mu\text{m}$  attenuation measurement would provide electron density measurements having the uncertainties shown under " $\nu$  measured" in Table 1. The final column shows the uncertainty in measured values of  $n_e \sim 3 \times 10^{10} \text{ cm}^{-3}$ . If  $\nu$  can be measured at somewhat higher pressures and/or electron densities, these errors would be correspondingly reduced.

### 2.3 Generation of Probe Wavelengths

Both of the above transitions can be optically pumped using the 9.6  $\mu\text{m}$  band of  $\text{CO}_2$ ; the 496  $\mu\text{m}$  by the P(20) line and the 1220  $\mu\text{m}$  by the P(32) line. These were originally obtained cw by Chang et al.<sup>2</sup>, who excited a 77 cm open, hole-coupled cavity with 6 mW of pump power. Collins<sup>3</sup> further developed the systematics of these transitions, using a 1.2 m open cavity with 2 mm hole-coupling and 30 watts of cw pump power, an arrangement quite similar to our second FIR cavity design.

For use as a spatially resolved probe beam, the hole-coupled outputs are severely limited by the diffraction limited beam divergence angle, which is inversely proportional to hole diameter. A 2 mm coupling hole produces a 200 mradian divergence angle, which leads to intolerable loss of intensity in our application. One needs a large diameter output window which is partially transmitting at 496  $\mu\text{m}$  and 1220  $\mu\text{m}$ . This is readily achieved using a wire mesh of appropriate grid spacing. The difficulty is that the cross-section of the  $\text{CH}_3\text{F}$  molecule for absorbing the  $\text{CO}_2$  pump radiation is rather small, requiring that the pump radiation make many passes through the FIR cavity to produce an inversion. One solution is to use intense pulsed optical pumping. At higher pumping rates, greater rates of collisional deactivation can be tolerated. This allows larger pressures of  $\text{CH}_3\text{F}$  with correspondingly shorter absorption lengths. Thus Brown et al.<sup>4</sup> used transverse optical pumping to obtain

500 W of pulsed output at 496  $\mu\text{m}$ . Drozdowicz et al.<sup>5</sup> used a similar approach in an oscillator-amplifier configuration to obtain 6 kW of peak output. However, pulsed output was of little use to us because of the great difficulty of measuring attenuation to one part in  $10^4$  on a pulsed basis. DeTemple and Danielewicz<sup>6</sup> found a solution appropriate to low power cw pumping. They developed a hybrid output mirror consisting of a metal mesh photolithographically deposited on a Si substrate, overcoated with a four layer dielectric coating. The FIR reflectivity could be varied by changing the grid parameters; the dielectric coating was transparent to the FIR radiation, while reflecting >98% throughout the  $\text{CO}_2$  laser bands. Using this output window to terminate a 1.2 m by 22 mm diameter dielectric waveguide cavity, they obtained 3 mW of cw output at 496  $\mu\text{m}$  from 8 watt of  $\text{CO}_2$  pump power, with a 28 mrad beam divergence--essentially the diffraction limited spread for a 22 mm aperture. Since this performance very closely matched our requirements and equipment capability, we adopted this approach during the latter part of the contract.

To obtain an FIR output having adequate stability for use as a diagnostic measurement, DeTemple and Danielewicz found it necessary to stabilize the frequency of the  $\text{CO}_2$  pump laser. To appreciate this necessity, we briefly examine the systematics of the 496  $\mu\text{m}$  transition in  $\text{CH}_3\text{F}$ . The lowest frequency vibrational mode of the  $\text{CH}_3\text{F}$  molecule, corresponding to C-F stretching and designated  $\nu_3 = 1$ , gives an absorption band centered near 9.54  $\mu\text{m}$ . The  $\text{CO}_2$  P(20) line at 9.55  $\mu\text{m}$  overlaps the subband Q(12,2) ( $\nu_3 = 0 \rightarrow 1$ ,  $J = 12 \rightarrow 12$ ,  $K = 2 \rightarrow 2$ ) of this absorption spectrum, thus pumping FIR emission at 496  $\mu\text{m}$  on the rotational transition ( $\nu_3 = 1 \rightarrow 1$ ,  $J = 12 \rightarrow 11$ ,  $K = 2 \rightarrow 2$ ). According to Hodges and Tucker<sup>7</sup>, this absorption subband is offset from the P(20) line center by 43 MHz, and has a Doppler broadened FWHM of 67 MHz at 300°K.

The  $\text{CO}_2$  pump laser will oscillate, not at P(20) line center, but at the axial cavity resonance frequency closest to line center. For our cavity, the axial resonance spacing is 38 MHz. Thus, if the cavity length is not dynamically tuned, a linear rate of change in either cavity

length or medium refractive index (affected by the intensity of electrical excitation in the medium) will cause an offset in pump frequency from P(20) line center which varies periodically between about -19 and +19 MHz. Figure 5 illustrates the resulting variation in CH<sub>3</sub>F excitation, assuming a FWHM of 67 MHz for the pump beam (typical, but not measured for this particular laser). The absorption spectrum of the CH<sub>3</sub>F, Q(12,2) branch is shown on the right, and the CO<sub>2</sub> P(20) emission spectrum on the left. In 5(a), illustrating the maximum negative offset of the P(20) emission, the overlap product (proportional to CH<sub>3</sub>F excitation rate), shown cross-hatched, has a peak value of 0.31. In 5(b), drawn for maximum positive offset, the overlap peak value is 0.84. Thus the CH<sub>3</sub>F, Q(12,2) excitation rate may vary periodically by a factor of 2.7. Since the FIR oscillation will be near threshold, the resulting periodic variation in FIR output can be even more, making it unsuitable for the FIR attenuation measurement.

The solution adopted by DeTemple and Danielewicz was to control the cavity length piezoelectrically with a commercial lock-in stabilizer which kept the pump frequency within about 2 MHz of P(20) line center. The method is discussed in Section 3.1.2.

#### 2.4 Choice of Equipment

The essential items of equipment are; a CO<sub>2</sub> pump laser operating cw on either the P(20) or P(32) lines of the 9.6 μm band, a suitable FIR generation cavity including provision for axial length tuning, and a FIR detector having adequate sensitivity to provide a S/N ratio >10<sup>4</sup> in the final attenuation measurement.

Our pump laser was adapted from an existing Coherent Radiation Laboratories Model 41 laser rated at 300 watt total cw output. With the addition of a suitable grating, 65 watt of multimode output was available at P(20), or a similar amount at P(32). Although the measured output power appeared to be sufficiently stable in time, the resulting FIR power generation was found to vary with time to an unacceptable degree because of variation of the pump frequency. Attempts to eliminate this

variation (see Section 3.1.2) by active stabilization of the pump cavity length were not successful. No suitable alternative pump laser was available within the company. At the time this deficiency was established, neither the remaining time nor the remaining contract funding were sufficient to permit obtaining a frequency stabilized source from outside the company. The use of a pump laser which could not be locked to a stable ( $\pm 2$  MHz) frequency was the principal cause of our failure to meet the contract objectives.

For a FIR generator cavity, we adapted an existing Advanced Kinetics model FIRML-475 HCN laser. This provided an Invar optical bench with suitably adjustable mirror mounts, one of which afforded linear motion at rates suitable for length spectroscopy at 496  $\mu\text{m}$  and 1220  $\mu\text{m}$ , plus an enclosure of sufficient flexibility to permit easy conversion to different cavity lengths and mirror arrangements for both open cavity and dielectric waveguide configurations. Although some difficulties were experienced with vacuum integrity and mechanical problems with the linear drive, these were overcome.

The detector system chosen for electron density measurement was an InSb detector operated at 4°K, also from Advanced Kinetics. The nominal system detectivity was adequate to provide  $S/N \geq 10^4$  at either 496  $\mu\text{m}$  or 1220  $\mu\text{m}$ , for a 5 mW diffraction-limited FIR beam of 2.5 cm generator exit aperture, after passage through the electron density measurement configuration described in Section 3.2.1. During all of the FIR generator development efforts described below, a pyroelectric detection system (Molelectron, type P3-00) was substituted which operated at ambient temperatures, thus simplifying the experimentation.

### 3. EXPERIMENTAL WORK

#### 3.1 FIR Generator Development

The sequence of FIR generator cavities investigated is summarized in Table 2. Our initial approach consisted of open cavity, hole coupled output resonators, discussed in detail in Section 3.1.1 following. This approach eventually provided 0.5 mW of output at 496  $\mu\text{m}$ , using 50 W of multimode pump power at P(20). However, the cavity gain was apparently marginal so that;

- 1) the output hole-coupler diameter had to be 4 mm or less, implying that the FIR beam divergence would be too great to permit electron density measurements of the required sensitivity, and
- 2) the FIR cavity length had to be so precisely controlled, to stay above the threshold for oscillation, that it was difficult to maintain an FIR output for any useful length of time.

We decided that hole-coupled cavities were not likely to satisfy the needs of this application, and pursued the use of dielectric waveguide cavities with partially FIR transmitting output mirrors. This work is detailed in Section 3.1.2. Our initial cavity design provided 1.6 mW output at 496  $\mu\text{m}$  with quite acceptable beam divergence (determined by the 22 mm output window diameter), and sufficient excess gain that the FIR cavity length could be maintained within the limits required for oscillation. These characteristics would have been suitable for the planned electron density measurements, except that the FIR output intensity varied periodically in time due to variation in P(20) pump frequency, as discussed in Section 2.3. Our remaining efforts were directed toward achieving a stable output, which we never obtained.

### 3.1.1 Open, Hole-Coupled Cavities

Our initial generator configuration is sketched in Fig. 6. Sixty-five watts of multimode pump beam, at either P(20) or P(32) is inserted into the FIR cavity through a 2 mm hole, by means of an  $f = 50$  cm focusing mirror, a triangular prism, and an  $f = 7.5$  cm collimating mirror. This optical combination permitted a convergent input beam having sufficiently low power density at the ZnSe entrance window to prevent damage, but with sufficiently small divergence ( $\sim f/150$ ) from its waist at the entrance hole to be trapped within the 3.1 m cavity. The FIR cavity was a stable resonator configuration formed by two spherical mirrors of 7.5 cm diameter and 4.1 m radius of curvature. The output mirror could be translated axially at appropriate constant velocities for cavity length spectroscopy. It had a central coupling hole of 1 cm diameter, which would have provided an output beam divergence at  $496 \mu\text{m}$  appropriate to  $f/8$  optics. This output aperture was chosen so that the full FIR output could be utilized in the electron density measurement, because the greatest acceptance angle which can afford 1 cm spatial resolution over a 10 cm interaction length is approximately  $f/8$ . The detection system consisted of a 90 Hz chopper and a pyroelectric detector directly viewing the FIR output through a TPX window. The pyroelectric detector output was processed in a lock-in amplifier, and displayed on an oscilloscope and chart recorder.

The FIR generator envelope, which was essentially unchanged from the HCN laser cavity used previously, was found to leak badly. The leakage rate had to be relatively low because the optimum  $\text{CH}_3\text{F}$  pressure for  $496 \mu\text{m}$  generation was expected to be  $\sim 0.04$  Torr. Generation of  $1220 \mu\text{m}$  radiation called for an optimum  $\text{CH}_3\text{F}$  pressure  $\sim 0.4$  Torr, and presented little problem. The leakage rate was reduced to a level that with continuous pumping permitted  $\text{CH}_3\text{F}$  pressure of 0.04 Torr with about 8% impurity content, and negligible impurity at  $\text{CH}_3\text{F}$  pressures exceeding 0.09 Torr.



Using this configuration we searched for FIR output over a range of  $\text{CH}_3\text{F}$  pressures, optical alignment refinements, etc. No output was seen at either wavelength. The output mirror was then replaced by a 4 m radius mirror having a 2 mm diameter coupling hole. Axial scanning spectrograms now showed a hint of output at each of the expected wavelengths; so weak that it was hidden in the noise level of the detector. By assuming the output wavelength and appropriately combining the data from long axial scans, we were able to infer output of several tens of  $\mu\text{W}$  at 496  $\mu\text{m}$  and 1220  $\mu\text{m}$ , respectively. Because the wavelength interval was forced, these statistical data cannot properly be interpreted as spectrograms, and are not reproduced here.

One probable contributing cause of this disappointing result was a severe alignment problem which came to light while aligning the following (1.4 m) cavity configuration. The problem was a mechanical fault in the axial scanning linkage which caused gross variation in the transverse alignment of the output mirror during axial scanning. Upon inspection, this proved to be an original equipment defect which we had been slow to suspect, because this drive had been successfully used by T. V. George to tune the HCN laser used in his earlier electron density measurements.<sup>1</sup>

Reviewing the failure of this resonator configuration, we recognized a number of deficiencies, as follows:

1. The original design had the pump beam entering with rather small divergence ( $\sim f/150$ ), on the assumption that 10 or more passes would fill the FIR mode volume with adequate uniformity of excitation. Considering the absorption coefficients given by Chang et al.<sup>2</sup> one finds that at the apparent optimum  $\text{CH}_3\text{F}$  pressures of 0.04 and 0.4 Torr, the  $\text{CO}_2$  beam is attenuated by about 20% and 35%, respectively, per pass through the 3.1 m path length. This results in most of the pump energy being absorbed in a narrow axial cone having diameters of about 5 mm at one end, and about 2 cm at the other, thus providing terrible excitation uniformity over the FIR mode volume.

2. Geometric ray tracing of the pump beam shows that, for any useful size output aperture, an excessive amount of pump energy is lost through the coupling holes on each end.
3. A problem related to 2) is an excessive intensity of CO<sub>2</sub> radiation falling on the TPX\* output window. When using the 1 cm coupling hole, we were forced to shield the central portion of the output window to prevent melting. This severely distorts the FIR output.
4. The leak rate of the original configuration was still excessive.

We next built the hole-coupled generator configuration sketched in Fig. 7, designed to surmount the above problems. The pump beam enters through a 5.5 mm (transverse projected diameter) hole in the plane mirror M1 and a 4 mm axial hole in the 4' m radius spherical mirror M2. The 1.4 m cavity is closed with a plane mirror equipped with axial scanning drive. The divergence of the entering pump beam (with its waist at M2) is tailored to be contained within a cylinder of 6 cm diameter, and to provide fairly uniform excitation over a cylinder of 3 cm diameter, roughly corresponding to the FIR mode volume. Simple ray tracing indicates that less than 6% of the pump beam is lost through M2 per double pass for the first five double passes. Due to diffraction at M2, over 90% of 496 μm radiation exiting through M2 is reflected by M1 through the TPX window, but essentially all pump radiation exiting through M2 also passes through M1. During the change to this configuration, the leakage rate was decreased to the point that the impurity level was negligible, although continuous pumping was still required when working at 496 μm.

---

\* TPX is the trademark of a methylpentene polymer having excellent characteristics for use as FIR lenses and windows.

The first attempts to generate 496  $\mu\text{m}$  with this cavity provided generally negligible output with erratically timed transient bursts of relatively high power as the FIR cavity length was scanned. These resulted from accidental coincidence of an FIR cavity axial length resonance of the  $\text{CO}_2$  pump with temporary transverse alignment of the wobbling mirror M3. Once the length scanning linkage was repaired, we obtained 0.5 mW of output at 496  $\mu\text{m}$ , using about 50 watts of multi-mode pump power at P(20). Oscillation at 496  $\mu\text{m}$  was obtained over a range of  $\text{CH}_3\text{F}$  pressures from 0.009 to 0.016 Torr. This pressure range being lower (and narrower) than the 0.04 Torr optimum seen by Collins<sup>3</sup> under similar conditions would indicate either a lower pumping rate or higher collisional deactivation rates. The latter could arise from impurities. Figure 8 is a spectrogram of total FIR power emitted versus cavity length, at a  $\text{CH}_3\text{F}$  pressure of 0.012 Torr. One sees four geometric modes, having identical wavelength (to 1 part in 300) of  $494 \pm 3 \mu\text{m}$ . The extreme narrowness of the resonant range in cavity length ( $\approx 0.02$  wavelength) suggests that the gain is very close to threshold.

Because of the narrow resonant range in cavity length, it proved very difficult to maintain the cavity on resonance for any useful length of time. This could be done with piezoelectric feedback tuning of the FIR cavity length, assuming a sufficiently constant pumping rate. However, the apparently marginal gain indicated that the output coupling hole could not be much enlarged over the present 4 mm diameter, which produces excessive beam divergence for efficient use in the planned electron density measurements. During this month, we had become aware of a far superior cavity configuration developed by DeTemple and Danielewicz<sup>6</sup> at the University of Illinois. We consulted with them, and decided to pursue their dielectric waveguide approach, discussed in the following section.

### 3.1.2 Dielectric Waveguide Cavity

The use of a cw source (to permit measuring  $\alpha$  to one part in  $10^4$ ), combined with the desire for 1 cm transverse spatial resolution, virtually require an FIR output aperture  $\geq 1$  cm in diameter. We had concluded from our open cavity studies that a hole-coupled aperture of this size was not likely to be suitable. Clearly, a large aperture, partially transmitting mirror was called for.

For any one FIR wavelength in this range, a conducting mesh of appropriate grid spacing constitutes a suitable mirror having any desired transmission. Unfortunately, such a mesh will not reflect pump radiation at  $9.6 \mu\text{m}$ . Several solutions are possible:

1. The cavity can be designed so that pump radiation does not have to reflect from the FIR output mirror. Several workers have successfully utilized such schemes\*, but none of them appeared suitable for our particular conditions.
2. An overlay could be added to the conducting mesh which was transparent to FIR and reflective at  $9.6 \mu\text{m}$ .
3. In principle, a sufficiently thin metal film would be totally reflective at  $9.6 \mu\text{m}$ , and partially transmitting at the FIR wavelengths.

We inquired of outside suppliers, and within these laboratories about these possibilities. Although some investigation of the third possibility had been done outside Westinghouse, the results did not appear promising. We believed that the Westinghouse CRL had the capability to develop a hybrid mirror with a partially FIR transmitting mesh structure and an IR reflecting overlay, but that the development could not be done within the limits of this contract.

---

\* Most such schemes apply to high power pulsed pumping, where the large excitation rates permit greater  $\text{CH}_3\text{F}$  pressures (and correspondingly faster collisional deactivation); thus the linear absorption coefficients are larger, permitting single pass excitation. Pulsed pumping was not appropriate to our requirements. However, the use of off-axis  $\text{CO}_2$  reflection in Ref. 4 can be adapted to cw excitation. The additional optical complexity did not seem appropriate for our use.

During November, R. A. Hoffman of these laboratories brought to my attention that the hybrid mirror development had been elegantly achieved at the Electro-Physics Laboratory of the University of Illinois, under Professor Coleman. We immediately contacted him and received excellent cooperation, entering into a consulting agreement whereby they would advise us in the design of an FIR generator very similar to the design which they had successfully used at 496  $\mu\text{m}$ , and would supply us with the needed hybrid output mirrors.

The University of Illinois generator<sup>6</sup> consists of a 1.2 m long dielectric waveguide cavity constructed of 22 mm ID pyrex tubing terminated by two plane mirrors; a metal mirror with an axial entrance hole for the focused pump radiation and a hybrid output mirror. The hybrid mirror partially transmits the FIR energy, and totally reflects the 9.6  $\mu\text{m}$   $\text{CO}_2$  pump energy. This is achieved by using an inductive metal grid photolithographically deposited on a Si substrate to partially transmit the FIR. A four-layer dielectric mirror is deposited atop this grid, which reflects >98% throughout the  $\text{CO}_2$  laser bands. Using this system, the Illinois group had already demonstrated an output at 496  $\mu\text{m}$  from  $\text{CH}_3\text{F}$  of 3 mW, with 26 mr divergence. That performance would be entirely suitable for our electron density measurements. The pump radiation frequency was stabilized at P(20) line center by active piezoelectric length tuning of the  $\text{CO}_2$  cavity using a Lansing Model 80.214 lock-in stabilizer, which maintains line center frequency by actively maximizing the P(20) output intensity.

We converted the Advanced Kinetics HCN laser envelope into a dielectric waveguide cavity similar to the University of Illinois configuration, and initiated the purchase of a Lansing lock-in stabilizer and piezoelectric translator. Figure 9 is a sketch of the dielectric waveguide cavity generator. Pump radiation enters through a 3 mm axial hole in the left hand plane mirror. The hybrid mirror was designed to reflect >98% at 9.6  $\mu\text{m}$ , and to transmit  $\sim$ 45% at 496  $\mu\text{m}$  and  $\sim$ 16% at 1220  $\mu\text{m}$ , over a 38 mm active diameter.

Following initial alignment of this cavity, 1.6 mW of output was obtained at 496  $\mu\text{m}$ , using 50 watt of multimode pump power. The length tuning spectrogram is shown in Fig. 10. Note that strong oscillation now occurs over >10% of an incremental wavelength range, rather than <2% as in the hole-coupled open cavity. Thus it proved relatively easy to manually tune the cavity length to peak output. With the FIR cavity length fixed at peak output, the output power was found to vary cyclically between 1.6 mW and about 1/5 this power, with a period of about three minutes, as shown in Fig. 11. This behavior did not correlate with any observable changes in total pump power, mode structure or pump beam alignment. The spectrum analyzer indicated that the full pump output remained on the P(20) line. It was assumed that the P(20) oscillation frequency was following the resonant frequency of the  $\text{CO}_2$  laser cavity, which was varying cyclically with an amplitude of 38 MHz due to thermal drift in the cavity length at the rate of about 10  $\mu\text{m}$  per three minutes. This would produce a three minute oscillation in the  $\text{CH}_3\text{F}$  excitation rate due to the changing overlap between pump frequency and the  $\text{CH}_3\text{F}$  absorption spectrum, as outlined in the introduction. Similar behavior had been noted at the University of Illinois (less seriously, because their  $\text{CO}_2$  laser was inherently more stable), and had been solved with the Lansing stabilizer system. Clearly, our time varying 496  $\mu\text{m}$  output was not suitable for the planned electron density measurements; the pump laser frequency would have to be stabilized.

Shortly thereafter, the hybrid mirror apparently deteriorated. We saw the peak 496  $\mu\text{m}$  output decline gradually from the value shown to essentially zero in the course of an afternoon, with no change in measured pump laser parameters. Variation over the full range of FIR cavity parameters,  $\text{CH}_3\text{F}$  pressure, etc., could not restore any significant FIR output. Subsequent examination of the output mirror showed a faint cloudy spot covering exactly the area corresponding to the waveguide diameter. The transmission and reflection of the mirror were measured at 9.6  $\mu\text{m}$  and 496  $\mu\text{m}$ . The mirror was cleaned, first with detergent solution, which had little effect, and then with chloroform followed by

distilled water, which appeared to remove the cloudy spot. Following cleaning, the FIR reflection and transmission values were unchanged. The results are roughly consistent with the nominal design values, and do not show any evidence of damage. Not being certain whether this mirror was in fact functionally degraded, we arranged to obtain two more hybrid mirrors from the University of Illinois. These had 333 and 500 mesh per inch, respectively (the original mirror was 500 mesh), and active areas of 50 mm diameter, for possible use in a 48 mm waveguide for 1220  $\mu\text{m}$  generation.

During March, the Lansing stabilizer system was received and installed. The output mirror of the CRL 41 pump laser was replaced with a window, and the piezoelectric translator carrying the output mirror was mounted externally, allowing enough space to insert a circular iris to force oscillation in fundamental mode. In this configuration, we could obtain 50 watt multimode at P(20), and 8 watt in fundamental mode with the iris in place.

The Lansing stabilizer works as sketched in Fig. 12. The  $\text{CO}_2$  cavity output mirror is held by a piezoelectric assembly of twelve elements in series. A 520 Hz AC voltage impressed across two elements produces a 520 Hz cavity length excursion of up to 2  $\mu\text{m}$  peak to peak. As the cavity length passes through a resonance with the center frequency of the spontaneous P(20)  $\text{CO}_2$  emission, the emitted power passes through a maximum. The resulting 520 Hz modulation of the pyroelectric detector, after passage through a tuned amplifier, is compared with the original 520 Hz signal. The difference in phase measures the magnitude and sense of the piezoelectric extension necessary to produce a cavity length resonance equal to the spontaneous P(20) emission frequency. This phase difference produces an error signal which determines the rate of increase (or decrease) of the DC voltage applied to the remaining ten piezoelectric elements. Thus the DC value of piezoelectric extension maintains the cavity length resonance at the P(20) center frequency. When the DC extension reaches its maximum of 12  $\mu\text{m}$ , the DC voltage is automatically reduced an amount equivalent to 1/2 wavelength, and the cavity length is locked to the adjoining axial resonance.

When the stabilizer system was applied to our CO<sub>2</sub> laser, the detector output resembled Fig. 13. The 520 Hz modulation in output power, though well developed, was accompanied by longer variations at 120 Hz and at lower, ill-defined frequencies. The 120 Hz must derive from gain changes due to discharge current supply instability. The source of the lower frequency variation is not known. The stabilizer was not able to determine a definite phase relationship between the 520 Hz output modulation and the reference signal, and thus could not lock on to the desired cavity length. We attempted to recondition the pump laser current supply as well as possible in the time available, but were never able to achieve frequency stabilization of the pump laser.

Early in May, the new hybrid mirrors were received, and the 500 mesh mirror was installed. The cavity was excited, first with 8 watt of P(20) fundamental mode, and then with 50 watt of multimode power at P(20). No 496 μm output could be obtained, at any CH<sub>3</sub>F pressure, or through any refinement of cavity alignment. We then substituted the original hybrid mirror, with equally negative results.

### 3.2 Planned Electron Density Measurements

#### 3.2.1 In 10 x 10 x 10 cm COFFEE Discharge

The optical configuration for measuring electron densities within the Westinghouse COFFEE discharge module is indicated schematically in Fig. 14. The optical design was based on a 5 mW diffraction limited output from the 22 mm aperture of the dielectric waveguide cavity. Briefly, the FIR radiation is focused onto a 180 Hz mirrored chopper which alternately directs the radiation into a test path or a reference path. The test beam can be translated to pass through any desired location within the discharge volume. The translating mirrors M6, M7 and M8 are so mounted and articulated that the test beam path length remains constant during translation, and no re-alignment is required. The test and reference beams contain identical lenses, at identical distances. The total beam path length, from dividing chopper to the center of the COFFEE module, equals 84 cm for each beam. After exiting the test chamber,



the two beams are combined in a condensing cone, and pass to a liquid He cooled InSb detector. The detector response is amplified through a two channel lock-in amplifier, and recorded. In operation, the variable wedge attenuator is adjusted so that test and reference beam powers are equal at the detector, producing a null in the 180 Hz difference signal; then the discharge current is ignited and stabilized and the resulting electronic attenuation is read directly in the 180 Hz channel. A 10 Hz chopper in front of the collector is used optionally. When it is in use, the 10 Hz channel records beam power at the detector. The 10 Hz chopper is normally left open to maintain maximum S/N ratios in the difference channel.

With the lock-in amplifier gain held constant, the signal  $V_{10}$  observed in the 10 Hz channel is proportional to the beam power at the detector. If the null was exact, the signal  $V_{180}$  in the 180 Hz channel is exactly the power decrease at the detector due to electronic attenuation over the 10 cm path length, times the same constant of proportionality. Then  $\alpha = 0.1 V_{180}/V_{10}$ . To determine  $\nu$ , one simply repeats the measurement at the other wavelength, thus obtaining  $\alpha_1$  and  $\alpha_2$ . Then  $\alpha_1$  and  $\alpha_2$  are substituted into Eqs. (1) and (2) to give  $n_e$  and  $\nu$ .

The critical requirement on this experiment design is to minimize differences between the test and reference beam losses, which might arise from uncontrollable changes in FIR mode structure, vagaries in atmospheric attenuation, etc. The safest way to have done this would have been to use oversize optics, which intercepted all of the beam at all points along the path. This was impossible because of the required spatial resolution, mechanical constraints, and the degree of diffraction at these wavelengths. We chose the next best alternative, to keep the two beams optically identical. Subject to this requirement, the beam path was minimized, in order to maximize power received at the detector. The resulting estimated losses from all causes imply detected powers of  $I_0/360$  at 496  $\mu\text{m}$  and  $I_0/1200$  at 1220  $\mu\text{m}$ , where  $I_0$  is the power emitted by the FIR generator. For 5 mW FIR output, the resulting S/N ratios should be  $3 \times 10^5$  at 496  $\mu\text{m}$  and  $1 \times 10^4$  at 1220  $\mu\text{m}$ .

The required TPX lens were procured, and detailed design of all necessary parts was complete. Fabrication of parts continued until mid-May, when it became apparent that the electron density measurements would not be carried out.

### 3.2.2 Application to the High Power Laser Test Facility at NASA-Lewis

One goal of the contract was to apply the developed measurement technique to measuring electron densities in the 1 m wide cavity of the High Power Laser Test Facility at NASA-Lewis. Clearly, the wavelengths chosen to obtain the required sensitivity over a 10 cm path, cannot give 1 cm spatial resolution over a 1.5 m path. To obtain a rough estimate of the spatial resolution possible over a 1.5 m path length, using 496  $\mu\text{m}$  radiation, we again apply the far field relationship  $\theta = 1.2 \lambda/d$ . A lens of diameter  $d$  and focal length  $f$  is positioned to focus the FIR beam at the center of a tube 1.5 m long and of diameter  $D$ , where  $D$  is the spatial resolution to be determined. Then geometric optics requires  $f/d \geq 75/D$ . The diameter of the focal spot is then  $s = 2f\theta = 2.4 \lambda f/d \geq 9/D$ . That is,  $sD \geq 9 \text{ cm}^2$ . Requiring  $s \leq D$ , the spatial resolution is given by  $D^2 \geq 9 \text{ cm}^2$ , implying  $D \geq 3 \text{ cm}$ . The actual case of a Gaussian beam in the near field is more complicated, but the above conclusion will be roughly correct.

To confine a beam to 1 cm diameter over a 1.5 m path length requires a wavelength  $\lesssim 70 \mu\text{m}$ . In this region of the spectrum, appropriate FIR sources are rare. However, a 118  $\mu\text{m}$  emission from  $\text{CH}_3\text{OH}$  would provide a good compromise between spatial resolution and electronic sensitivity. This emission can be excited optically by  $\text{CO}_2$  laser with efficiency comparable to  $\text{CH}_3\text{F}$ . A 118  $\mu\text{m}$  beam can be confined to about 1.4 cm diameter over a 1.5 m path. The attenuation factor would be less than for 496  $\mu\text{m}$  by a factor of  $\omega^2 \sim 18$ , but since the path length would be 15 times greater, the sensitivity to electron number density would be almost as good as the values should in the earlier table.

The available options for measuring electron number density in the High Power Laser Test Facility are:

1. Use 496  $\mu\text{m}$  technique over  $\sim 1.5$  m path length to achieve spatial resolution to 3 cm.
2. Replace  $\text{CH}_3\text{F}$  with  $\text{CH}_3\text{OH}$ , and use 118  $\mu\text{m}$  radiation. to give 1.4 cm resolution, and 18 times poorer sensitivity.
3. Study a 10 cm transverse section of the laser volume, with better than 1 cm spatial resolution.

The first of these three options was pursued during this contract.

#### 4. REFERENCES

1. T. V. George and L. J. Denes, Appl. Phys. Lett. 26, No. 1, pp. 1-3 (1975).
2. T. Y. Chang, T. J. Bridges and E. G. Burkhardt, Appl. Phys. Lett. 17, No. 8, p. 249 (1970).
3. R. M. O'Connell, "Optically Pumped Methyl Fluoride and Methyl Alcohol Far Infrared Molecular Lasers", Graduate Thesis submitted to Dept. of E.E., Graduate College of the Univ. of Illinois at Urbana-Champaign (1972).
4. F. Brown, Infrared Physics 16, pp. 171-174 (1976).
5. Z. Drozdowicz, R. J. Temkin, K. J. Button, and D. R. Cohn, Appl. Phys. Lett. 28, No. 6, p. 328 (1976).
6. T. A. DeTemple and E. J. Danielewicz, IEEE J. Quant. Elect. QE-12, No. 1, pp. 40-47 (1976).
7. D. T. Hodges and J. R. Tucker, Appl. Phys. Lett. 27, No. 12, pp. 667-669 (1975).

## 5. ACKNOWLEDGEMENT

I wish to thank E. J. Manista of NASA-Lewis for his unstinting helpfulness as monitor of the contract, R. A. Hoffman of the CRL for bringing to my attention the work done at the University of Illinois, and P. D. Coleman and E. J. Danielewicz of the Electro-Physics Laboratory of the University of Illinois for much valuable advice. I am particularly indebted to E. J. Danielewicz for finding time in a busy schedule to promptly fabricate the needed hybrid mirrors. I am also grateful to J. C. Brown and R. L. Grassel for intensive and intelligent assistance.

TABLE 1

## UNCERTAINTY IN MEASURED ELECTRON DENSITIES

Composition CO <sub>2</sub> :N <sub>2</sub> :He	Pressure (Torr)	$\frac{\nu}{\omega_1}$ <sup>(1)</sup>	Minimum detectable electron density <sup>(2)</sup> (10 <sup>8</sup> cm <sup>-3</sup> )		$\nu$ intrinsic <sup>(3)</sup>	$\nu$ measured <sup>(4)</sup>	Uncertainty in $n_e$ , 2 wavelengths measurement (10 <sup>8</sup> cm <sup>-3</sup> )	Error at $n_e = 3 \times 10^{10}$ (%)
			496 $\mu$ m	1220 $\mu$ m				
1:1:8	120	0.20	45.0	7.68	800	7.68 + 14%	16.6	
	280	0.38	24.5	4.49	108	4.49 + 11.5%	13.0	
	450	0.61	15.8	3.32	23	3.32 + 7%	8.1	
1:7:20	150	0.26	36.1	6.24	400	6.24 + 9.7%	11.8	
	280	0.48	19.8	3.82	52	3.82 + 7%	8.3	
	450	0.76	12.9	3.04	10	3.04 + 3%	4.0	

- (1)  $\nu$  calculated from gas conditions;  $\omega_1$  (1220  $\mu$ m) =  $1.5 \times 10^{12}$  sec<sup>-1</sup>.
- (2) i.e., the electron density which produces observed attenuation of  $10^{-4}$  over a 10 cm path.
- (3) Uncertainty in  $n_e$  calculated from attenuation measurements at two wavelengths via. Eq. (4), with no prior knowledge of  $\nu$ .
- (4) Calculating  $\nu$  via Eq. (2) from two wavelength measurements at 450 Torr,  $n \sim 3 \times 10^{10}$  cm<sup>-3</sup>, correcting  $\nu$  for pressure, and calculating  $n_e$  via Eq. (1) from observed 1220  $\mu$ m attenuation.

TABLE 2

## FIR GENERATOR CONFIGURATIONS INVESTIGATED

	Open Cavity				Dielectric Waveguide				
	6	6	7	7	9	9	9	9	9
Figure No.	6	6	7	7	9	9	9	9	9
Cavity Length (m)	3.1	3.1	1.4	1.4	1.2	1.2	1.2	1.2	1.2
Input Hole Dia. (mm)	2	2	(thru output)		3	3	3	3	3
Output Hole Dia. (mm)	10	2	4	4	22	(partially transmitting)			
Output Mirror Dia. (mm)	75	75	75	75	38	38	50	50	38
Deficient Features:									
Excessive Losses	X	X							
Non-Uniform Excitation	X	X							
Vibration in Output Mirror	X	X	X	X					X
Degraded Hybrid Mirror									X
Stabilizer in place, not locking on									X
Pump Power Input (W)	65	65	65	50	50	50	50	50	50
Multimode									
Fund. Mode							8	8	8
FIR Output Power (mW)	--	~0.01?	Erratic	0.5(a)	1.6(b)	--	--	--	--

NOTES: a) Oscillating too near threshold, plus excessive beam divergence  
 b) Suitable except for variation due to pump frequency oscillation

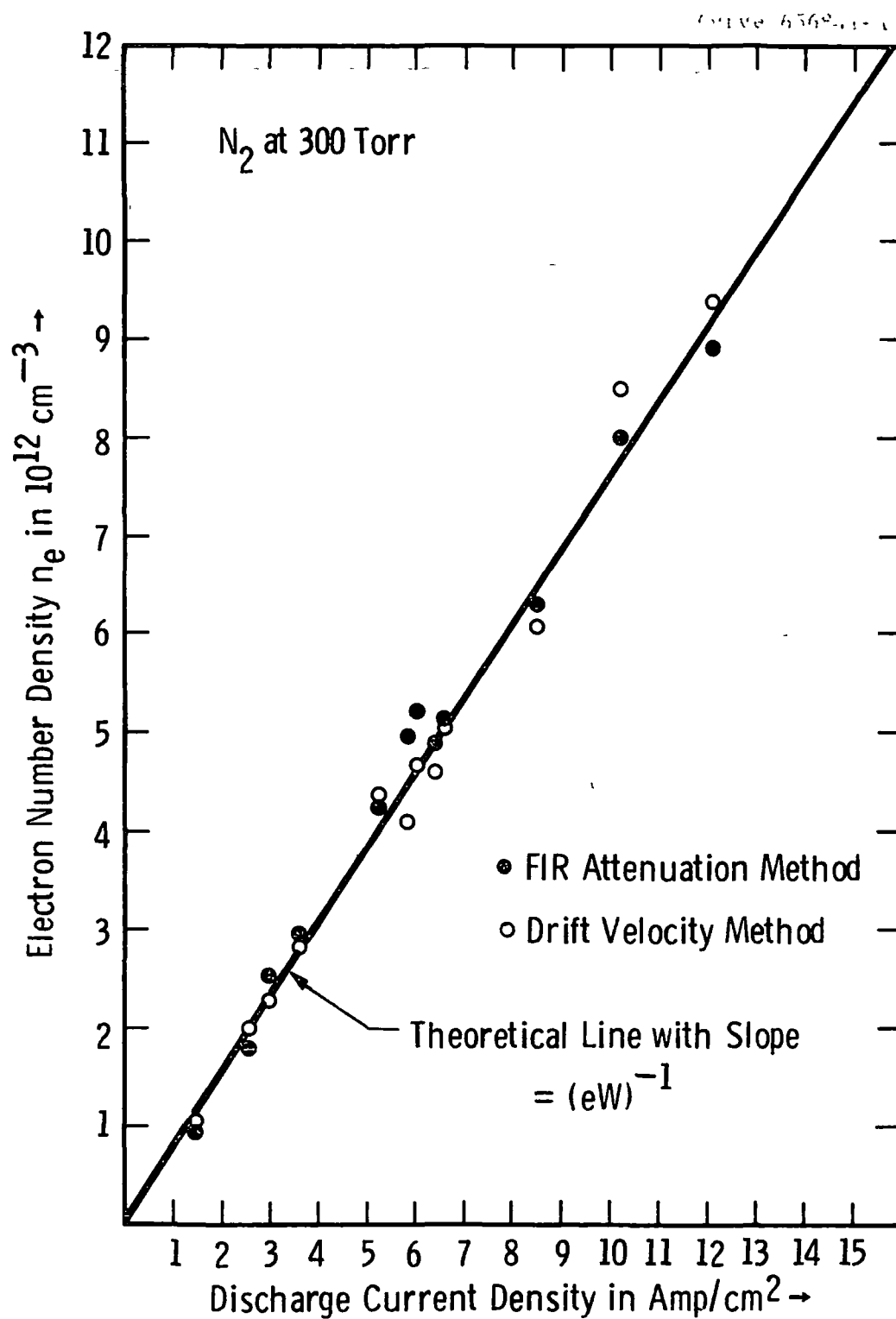


Fig. 1 - Comparison of electron densities measured by FIR attenuation and drift velocity methods in nitrogen



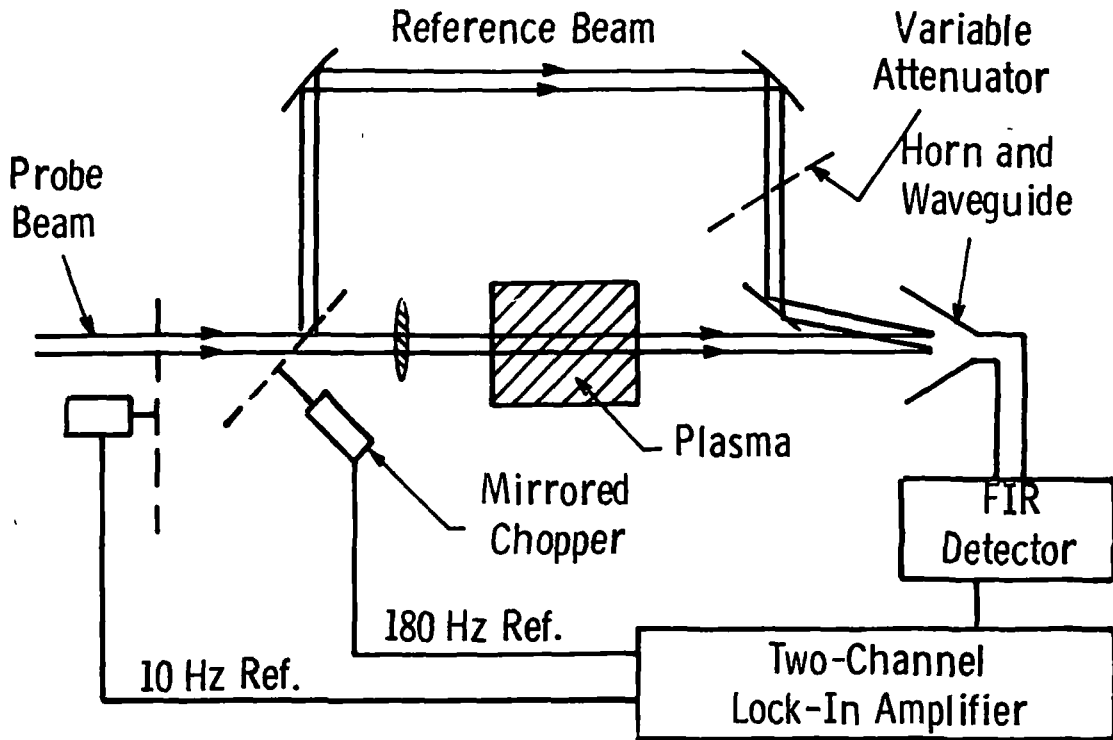


Fig. 2 — Principle of chopped, dual beam attenuation measurement. With no discharge, 180 Hz difference signal from detector is nulled with variable attenuator. Then with discharge established, 180 Hz difference signal measures attenuation.

Curve-687921-A

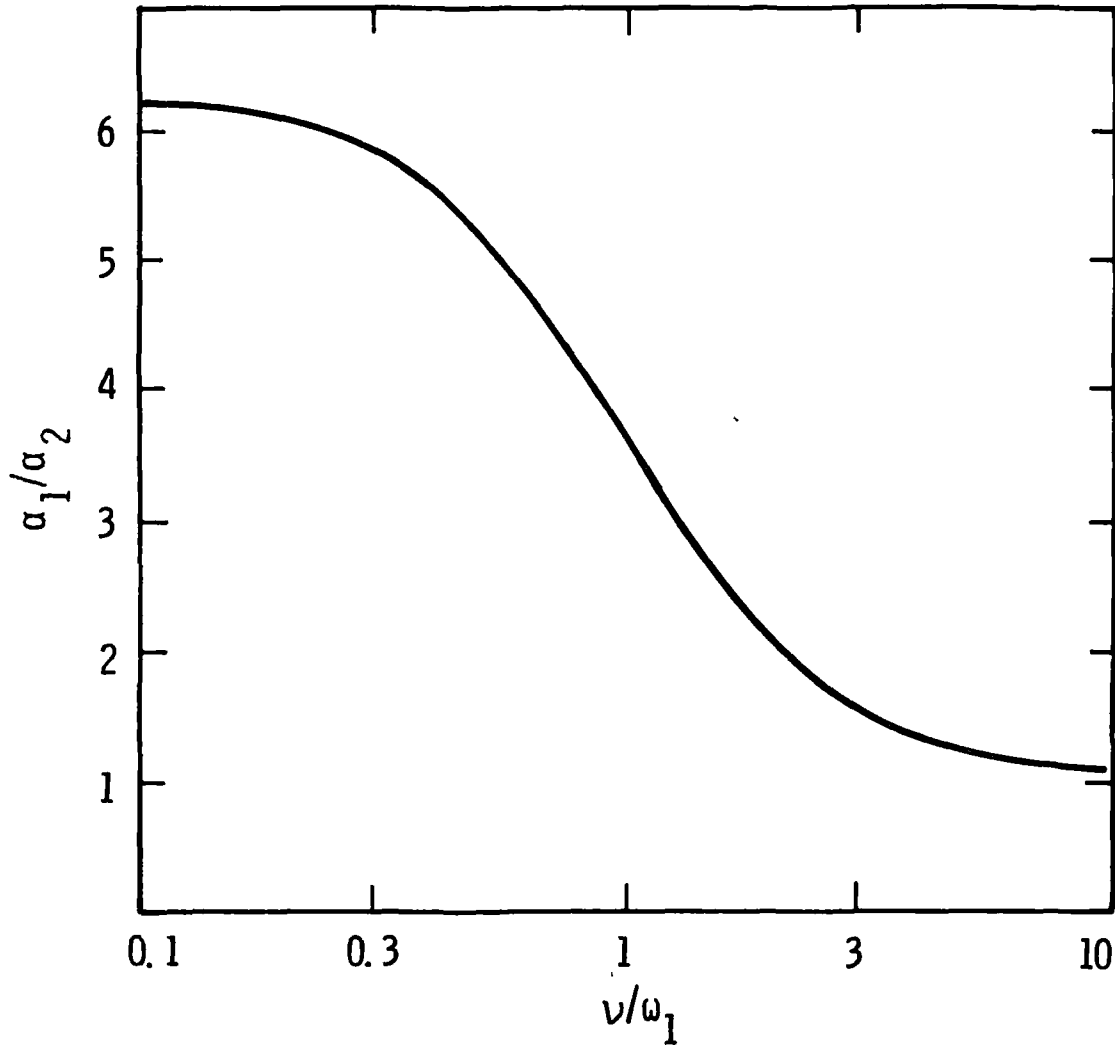


Fig. 3 — Ratio of attenuation constants for probe radiations at 1220  $\mu\text{m}$  ( $\omega_1$ ) and 496  $\mu\text{m}$  ( $\omega_2$ ) versus normalized collision frequency ( $\nu/\omega_1$ )

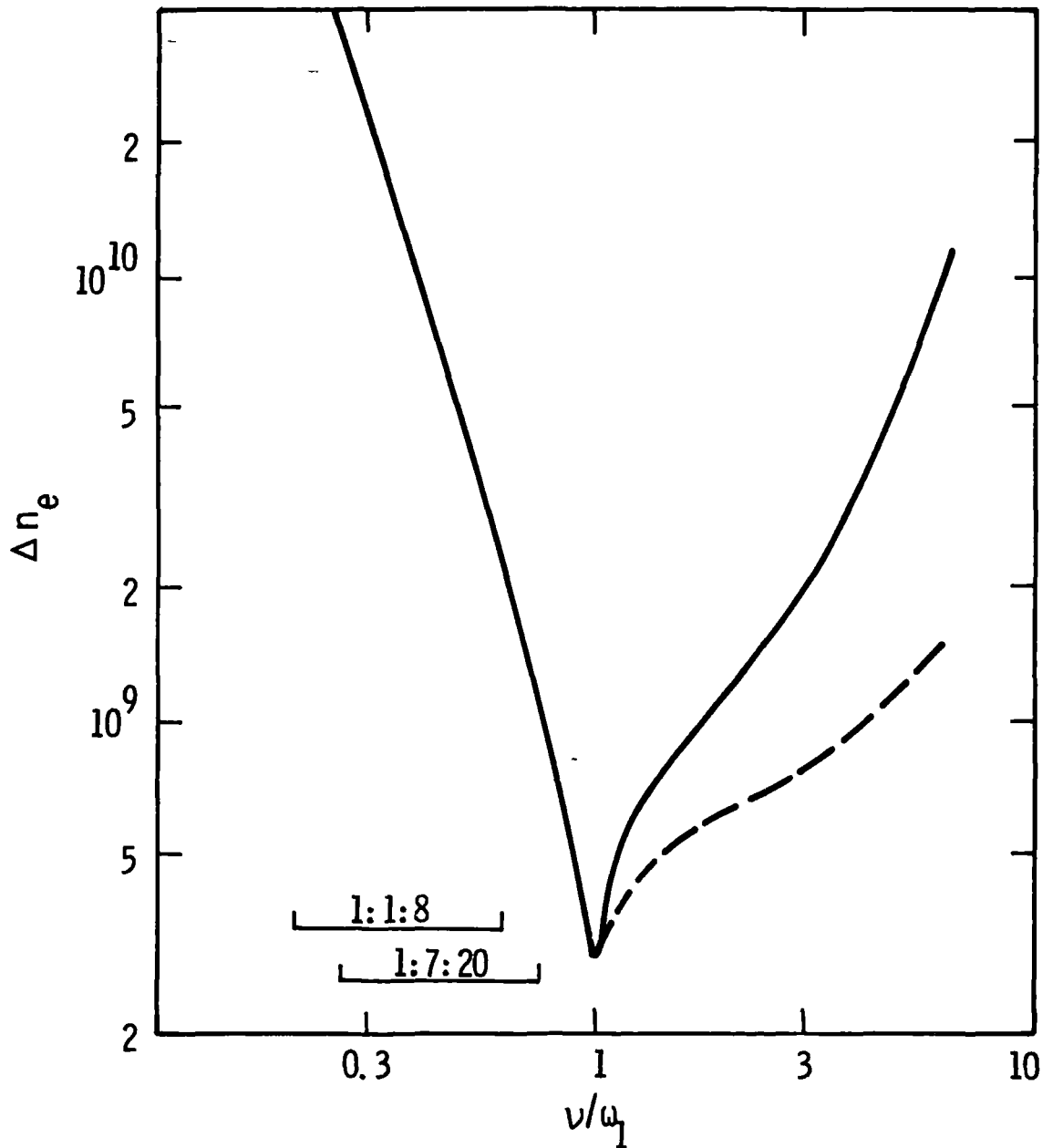


Fig. 4 - Uncertainty in measured value of  $n_e$ , using two probe frequencies to eliminate  $\nu$ , as a function of  $\nu$ . The horizontal bars indicate the expected range in  $\nu$  for the gas mixture specified.  $\omega_1 \times 1.5 \times 10^{12} \text{ sec}^{-1}$

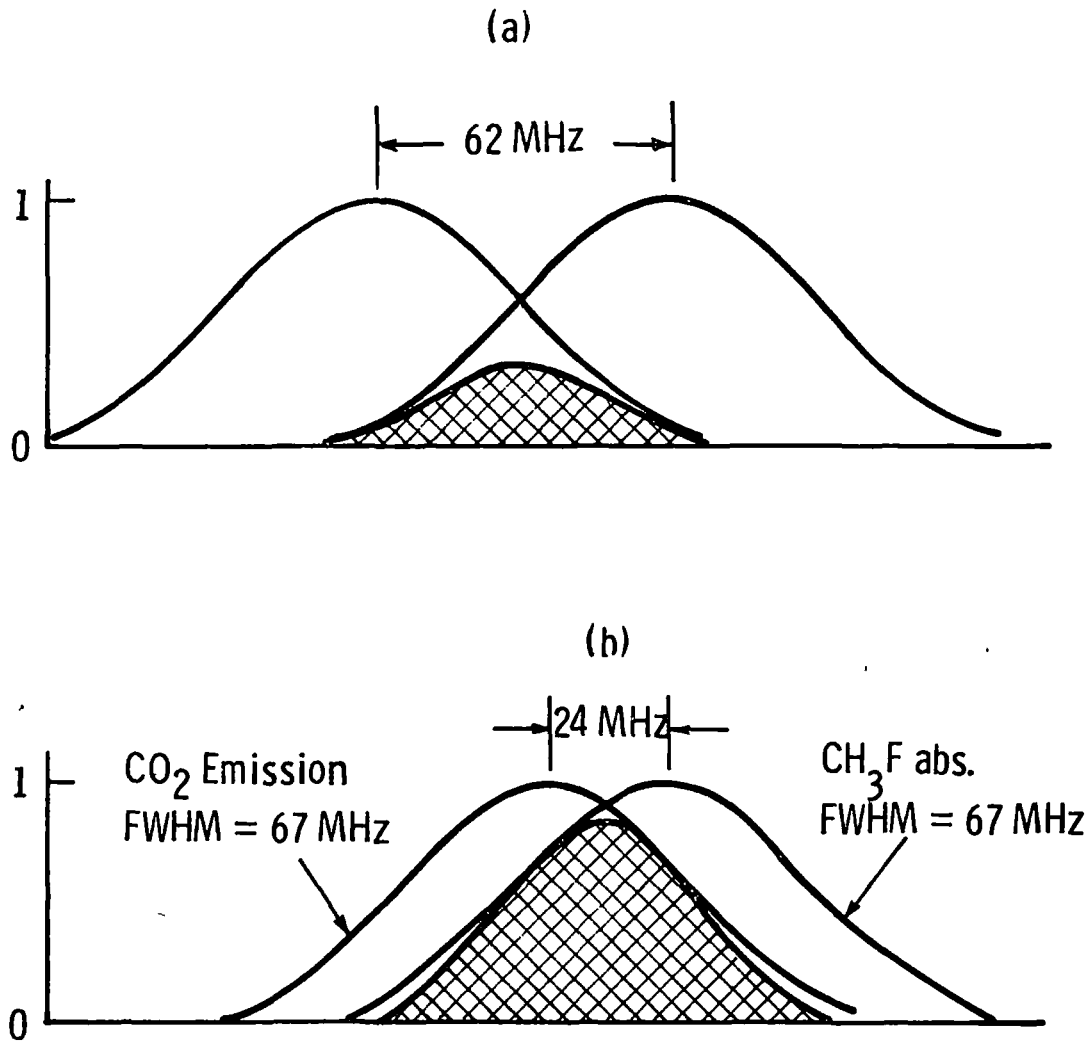


Fig. 5 — Overlap (crosshatched) between CO<sub>2</sub>, P (20) emission and CH<sub>3</sub>F, Q (12, 2) absorption for; (a) - 19 MHz offset of CO<sub>2</sub> emission from line center and (b) + 19 MHz offset.

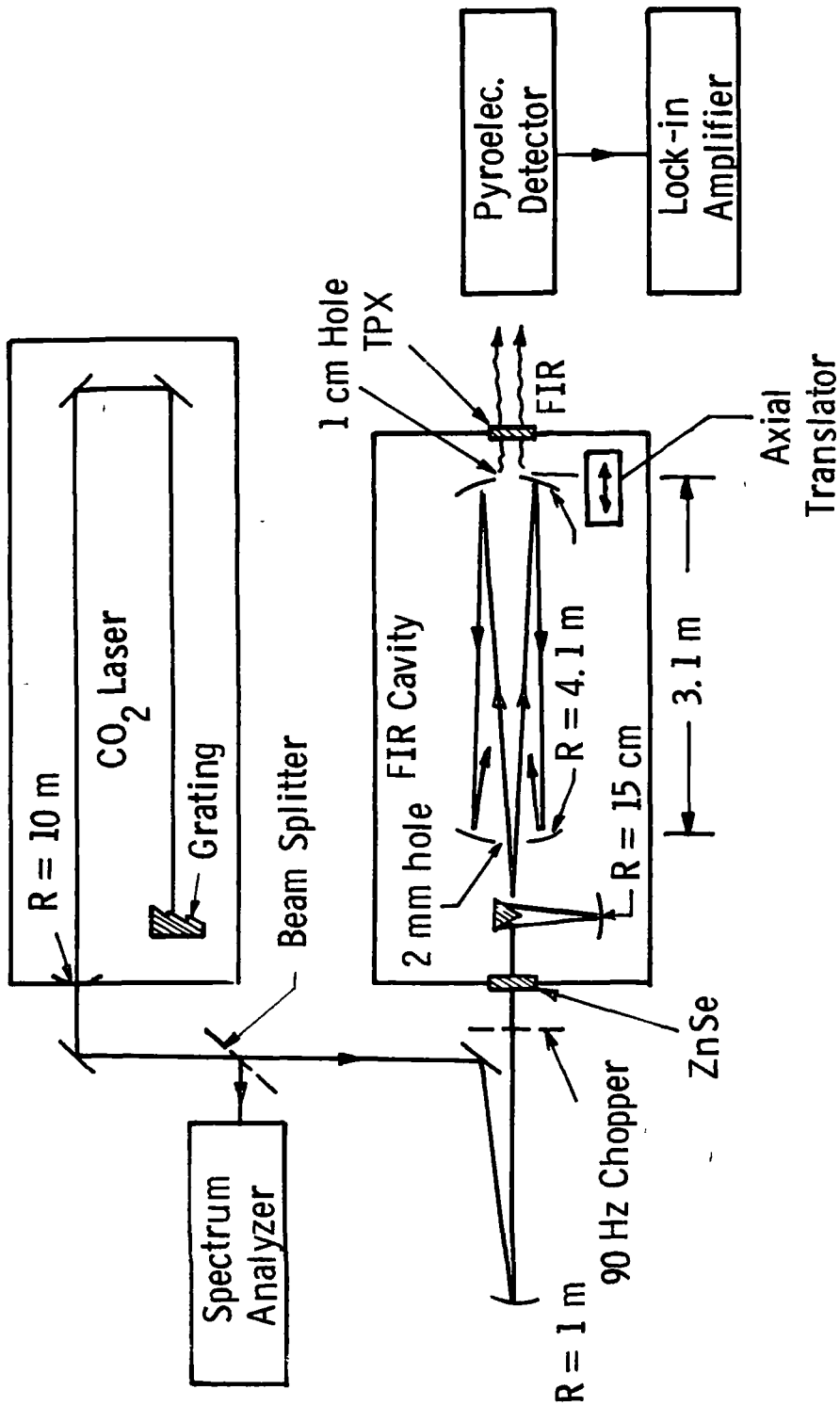


Fig. 6 - Schematic diagram of 3.1 m, hole coupled FIR generator

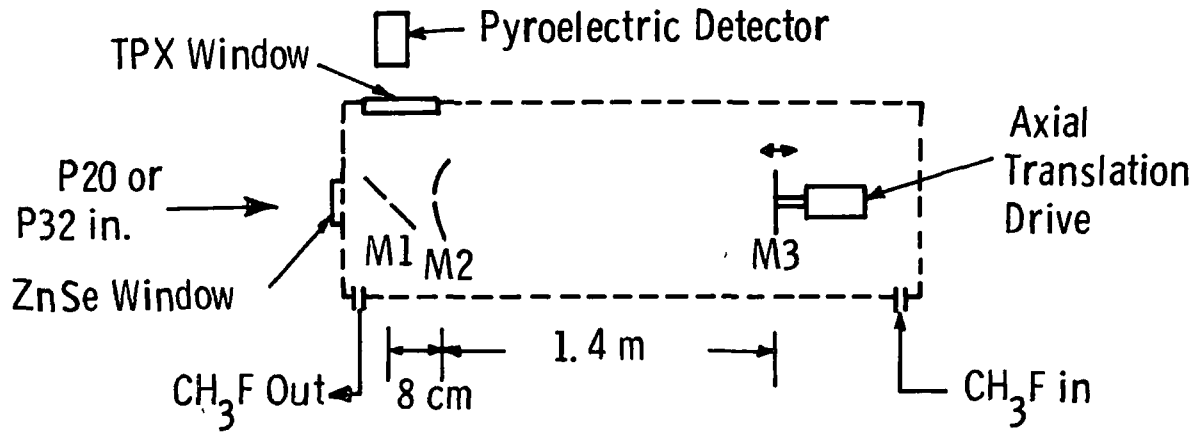


Fig. 7 - Open, hole-coupled FIR cavity. M1 is plane with 5.5 mm (projected) hole. M2 is 7.5 cm dia. with 4 mm dia. hole and  $r = 4$  m. M3 is a 7.5 cm dia. plane mirror.

Curve 687926-A

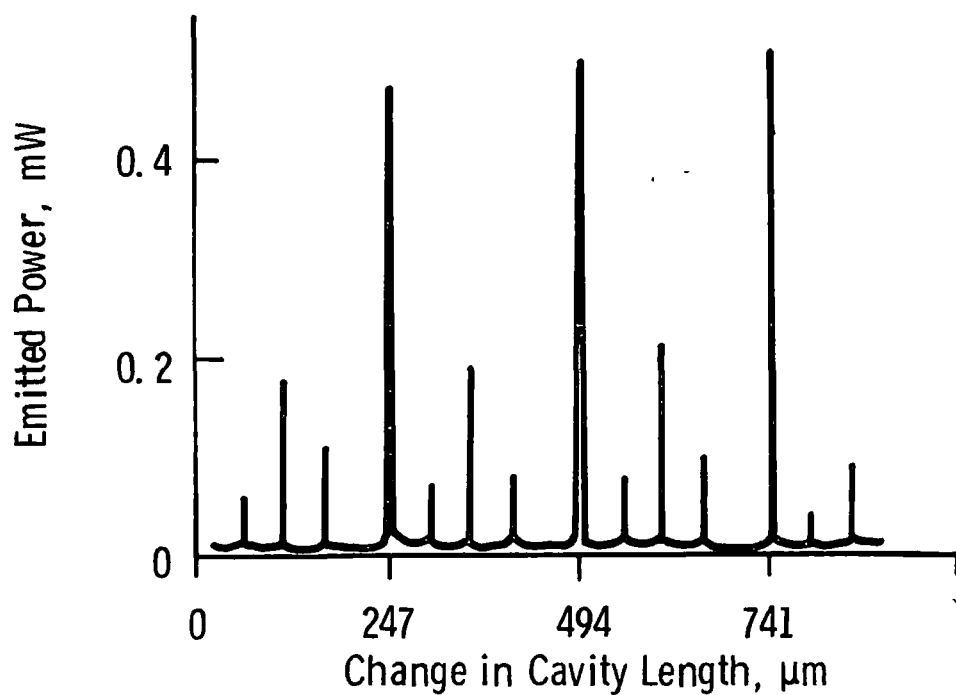


Fig. 8 — Emitted power at 496  $\mu\text{m}$  versus cavity length. Recorder time constant equivalent to 1.2  $\mu\text{m}$  of scan. Cavity configuration of Fig. 7.

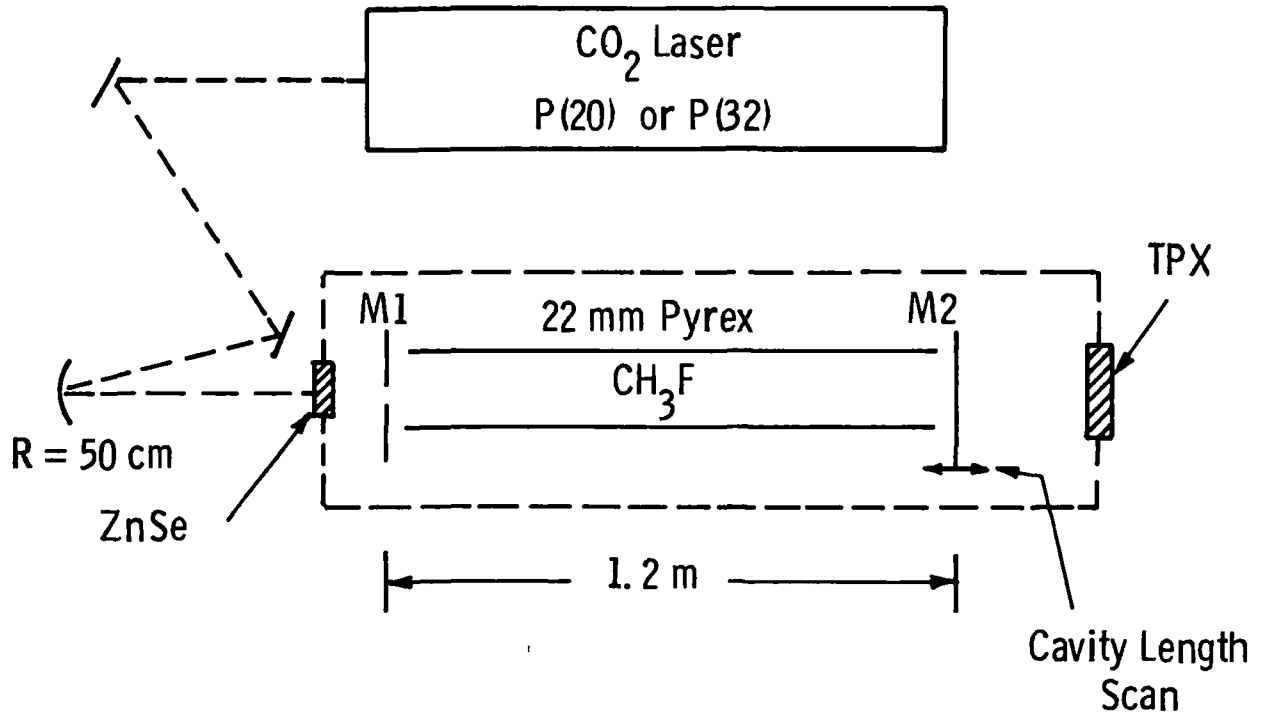


Fig. 9 — Dielectric waveguide cavity FIR generator. M1 is a plane mirror with a 3 mm diam. hole. M2 is a hybrid mirror transmitting ~10% at 1220  $\mu\text{m}$ , or ~28% at 496  $\mu\text{m}$ , and reflecting >98% at 9.6  $\mu\text{m}$ .



Curve 687923-A

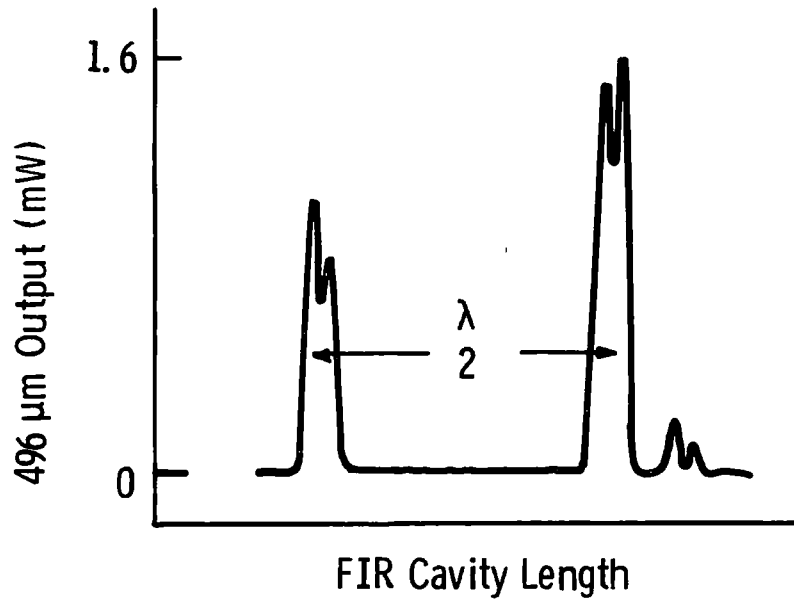


Fig. 10 — Cavity length tuning spectrogram of 496  $\mu\text{m}$  output from dielectric waveguide cavity sketched in Fig. 9.

Curve 687924-A

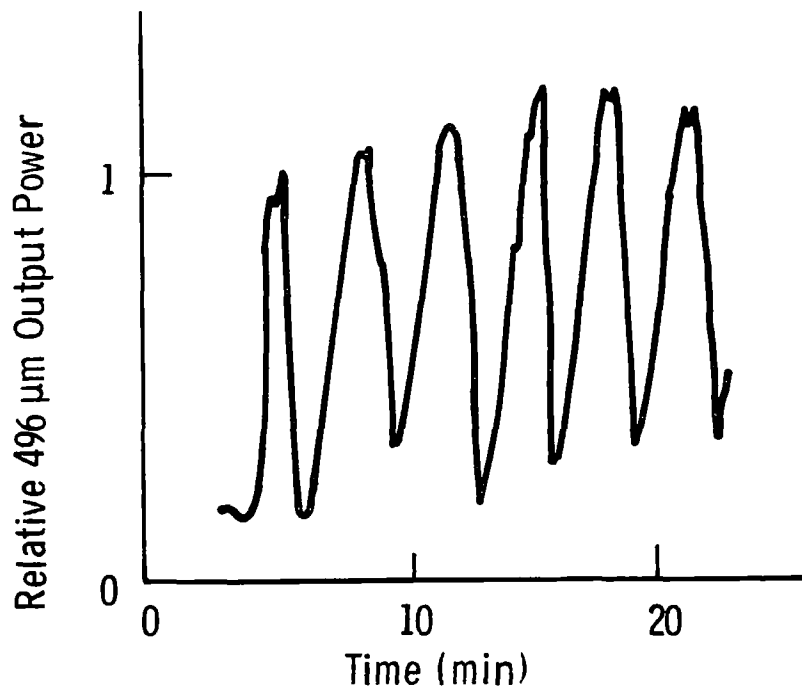


Fig. 11 — Temporal variation of 496 μm output with all controlled parameters held constant for cavity of Fig. 9.

Dwg. 6398A22

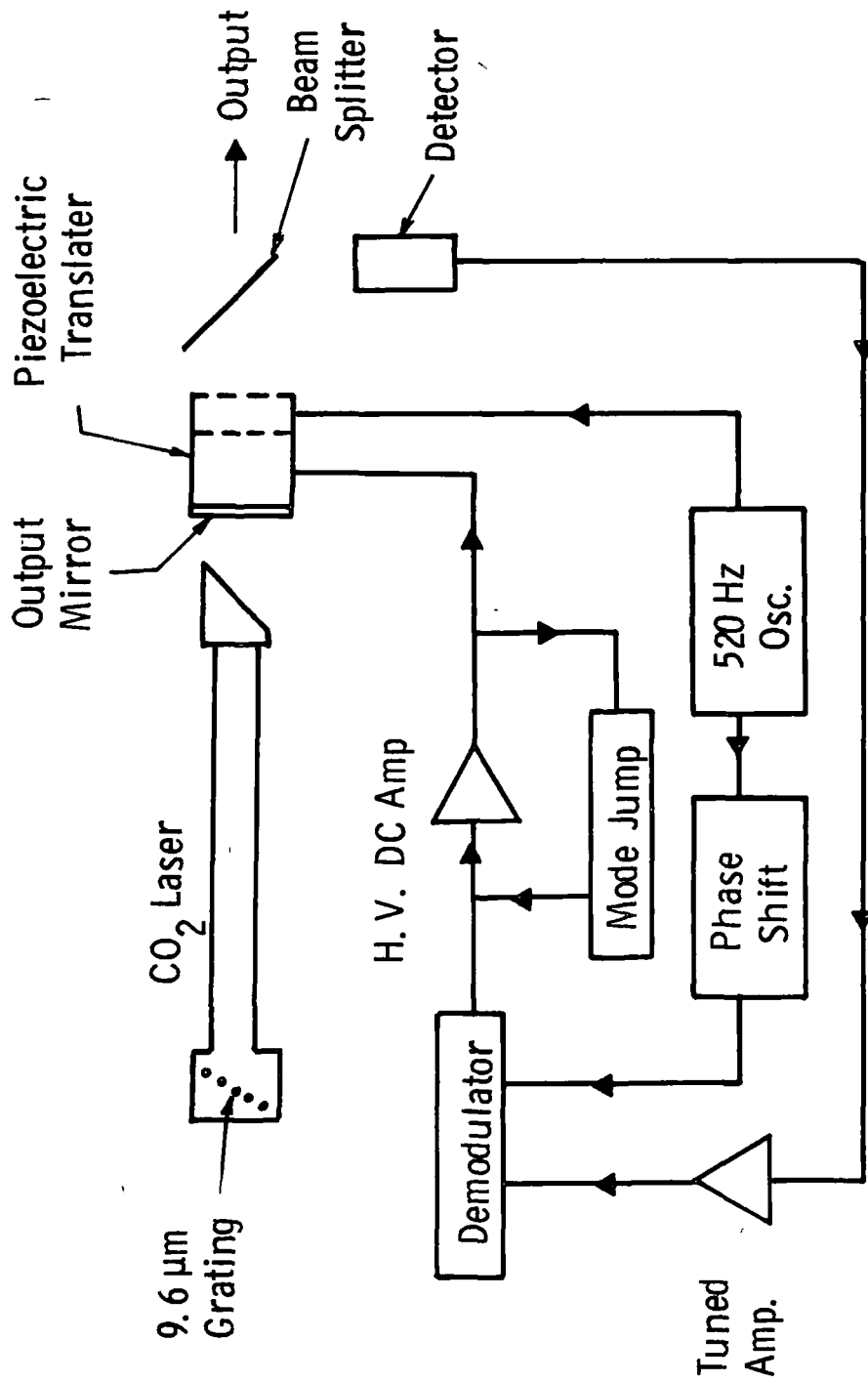


Fig. 12 - Block diagram illustrating operation of Lasing frequency stabilizer

Curve 687925-A

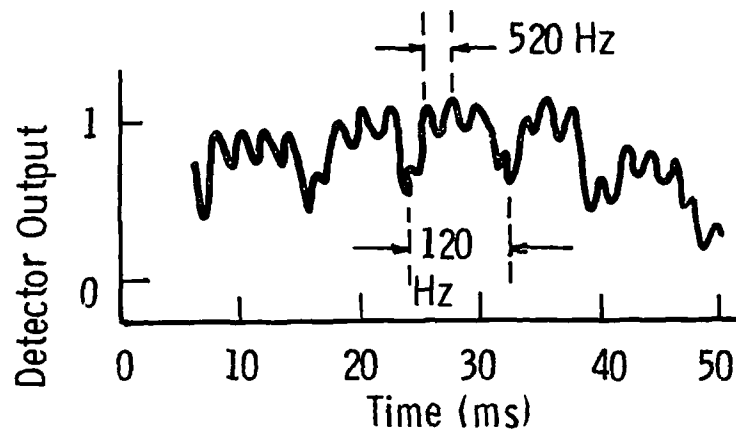


Fig. 13 - Observed modulation of CO<sub>2</sub> output power with 520 Hz cavity length modulation at maximum.

Dwg. 6398A18

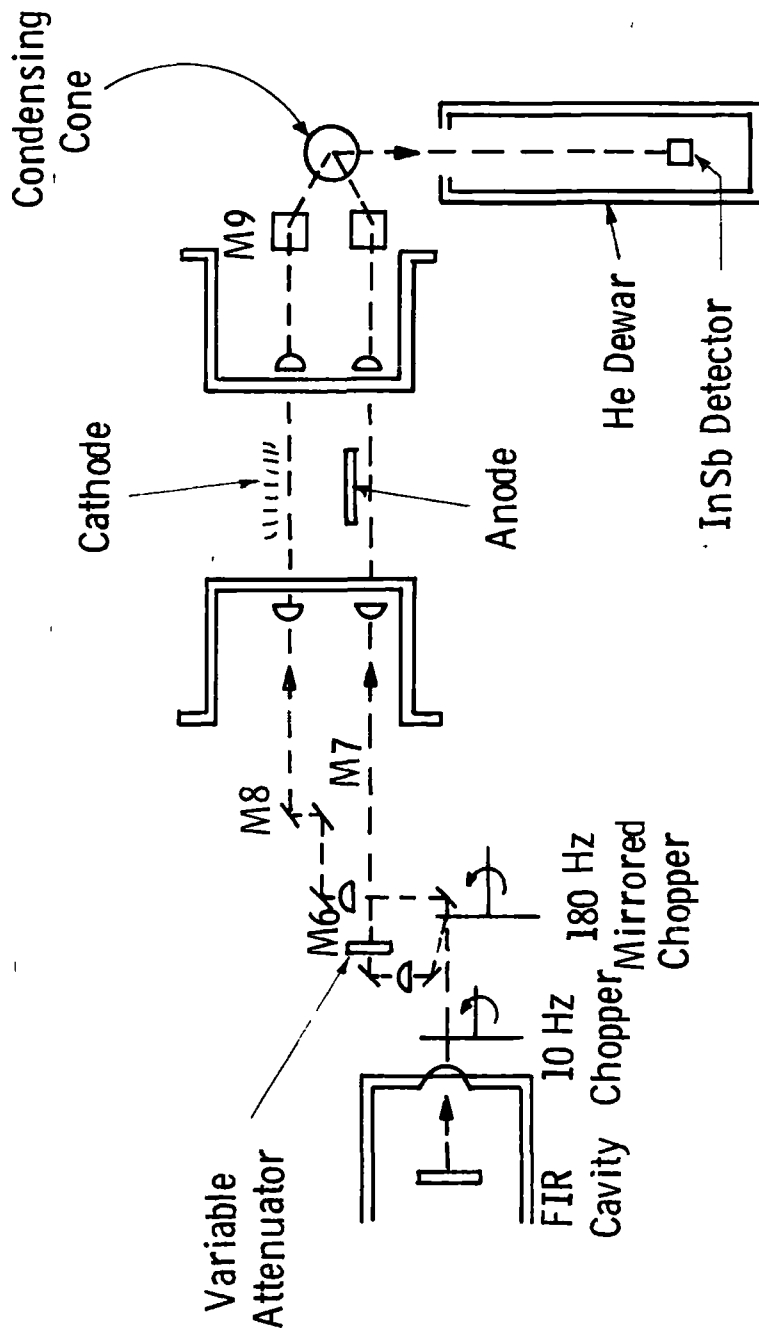


Fig. 14 — Optical configuration for measuring electron densities.  
Refer to text for details

DISTRIBUTION LIST FOR LASER FINAL REPORTS

1. National Aeronautics & Space Administration  
 Lewis Research Center  
 21000 Brookpark Road  
 Cleveland, Ohio 44135
  - Attn: Contracting Officer, MS 500-313 1
  - Technical Utilization Office, MS 3-16 1
  - Technical Report Control Office, MS 5-5 1
  - AFSC Liaison Office, MS 501-3 2
  - Library, MS 60-3 2
  - Office of Reliability & Quality Assurance,  
 MS 500-211 1
  - E.J. Manista, Project Manager, MS 500-318 5
  
2. National Aeronautics & Space Administration  
 Headquarters  
 Washington, D.C. 20546
  - Attn: Office of Aeronautics & Space Technology  
 Director, Space Propulsion & Power/RP 1  
 F. C. Schwenk/RR 1
  - Attn: Office of Manned Space Flight  
 Director, Advanced Manned Mission/MT 1
  - Attn: Office of Space Science  
 Director, Launch Vehicles & Propulsion/SV 1
  - Attn: Office of Technology Utilization Division  
 Director, Technology Utilization/KT 1
  
3. National Aeronautics & Space Administration  
 Ames Research Center  
 Moffett Field, California 94035
  - Attn: Library 1
  - Dr. Kenneth W. Billman 1

4. National Aeronautics & Space Administration  
Flight Research Center  
P. O. Box 273  
Edwards, California 93523  
Attn: Library 1
  
5. National Aeronautics & Space Administration  
George C. Marshall Space Flight Center  
Huntsville, Alabama 35912  
Attn: Library 1
  
6. National Aeronautics & Space Administration  
Goddard Space Flight Center  
Greenbelt, Maryland 20771  
Attn: Library 1
  
7. National Aeronautics & Space Administration  
John F. Kennedy Space Center  
Cocoa Beach, Florida 32931  
Attn: Library 1
  
8. National Aeronautics & Space Administration  
Lyndon B. Johnson Space Center  
Houston, Texas 77001  
Attn: Library 1
  
9. National Aeronautics & Space Administration  
Langley Research Center  
Langley Station  
Hampton, Virginia 23365  
Attn: Library 1  
R. Hess 1

10. NASA Scientific & Technical  
Information Facility  
Attn: Accessioning Department  
P.O. Box 8757  
Balt/Wash International Airport  
Maryland 21240 10
11. Jet Propulsion Laboratory  
4800 Oak Grove Drive  
Pasadena, California 91103  
Attn: Library 1  
G. R. Russell 1  
M. J. Cork 1  
G. Lewicki/180-700 1
12. Defense Documentation Center  
Cameron Station  
Building 5  
5010 Duke Street  
Alexandria, Virginia 22314  
Attn: TISIA 1
13. Air Force Rocket Propulsion Laboratory  
Edwards, California 93523  
Attn: Library 1  
D. A. Hart/XP 1  
C. Selph/LKCG 1  
F. B. Mead Jr./LKDA 1
14. Defense Advanced Research Projects Agency  
1400 Wilson Bl.  
Arlington, VA 22209  
Attn: Dr. Peter Clark 1  
Major G. Canavan 1
15. ODDR&E  
Pentagon  
Washington, D.C. 20301  
Attn: Dr. Robert Greenberg 1



16. Commander  
US Army Missile Command  
Redstone Arsenal, AL 35809  
Attn: Walter B. Jennings, Jr. 1
  
17. Director  
Ballistic Missile Defense Advanced Technology Center  
PO Box 1507  
Huntsville, AL 35807  
Attn: ATC-O Mr. W. O. Davies 1
  
18. Director  
US Army Ballistic Research Lab.  
Aberdeen Proving Ground, MD 21005  
Attn: Dr. Robert Eichelberger 1
  
19. Office of Naval Research  
495 Summer St.  
Boston, MASS 02110  
Attn: Dr. Fred Quelle 1
  
20. Office of Naval Research  
800 N. Quincy St.  
Arlington, VA 22217  
Attn: Dr. W. J. Condell (421) 1
  
21. Naval Missile Center  
Point Mugu, CA 93042  
Attn: Gary Gibbs (Code 5352) 1
  
22. Superintendent  
Naval Postgraduate School  
Monterey, CA 93940  
Attn: Library (Code 2124). 1

23. Commander  
 Naval Weapons Center  
 Attn: Mr. E.B. Niccum, Code 4011 1  
 China Lake, CA 93555
- 24.- Naval Research Lab.  
 Washington, D.C. 20375  
 Attn: Dr. P. Livingston (Code 5560) 1  
 Dr. J. L. Walsh (Code 5503) 1  
 Dr. J. T. Schriempf (Code 6410) 1
25. Naval Ordnance Lab.  
 White Oak  
 Silver Spring, MD 20910  
 Attn: Dr. Leroy Harris (Code 313) 1
26. Air Force Weapons Lab.  
 Kirtland AFB, NM 87117  
 Attn: Col. Donald L. Lamberson (AR) 1  
 Col. John C. Scholtz (PG) 1  
 Col. Russell K. Parsons(LR) 1  
 Col. Rose (AL) 1
27. Hq. SAMSO  
 PO Box 92960, Worldway Postal Center  
 Los Angeles, CA 90009  
 Attn: Capt. Dorian A. DeMaio (XRTD) 1
28. AF Avionics Lab. (TEO)  
 Wright Patterson AFB, OH 45433  
 Attn: Mr. K. Hutchinson 1

29. AF Materials Lab.  
Wright Patterson AFB, OH 45433  
Attn: Maj. Paul Elder (LPJ) 1
  
30. AF Aero Propulsion Laboratory  
Wright Patterson AFB, OH 45433  
Attn: Maj. George Uhlig (AFAPL/MA) 1
  
31. RADC (OCSE)/Mr. R. Urtz  
Griffiss AFB, NY 13441 1
  
32. Hq. Electronics Systems Div. (ESD)  
Hanscom AFB, MA 01731  
Attn: Capt. Allen R. Tobin (XRE) 1
  
33. Air University  
Institute for Professional Development  
Maxwell AFB, Alabama 36112  
Attn: ACSC/EDCS 1
  
34. Aerojet Liquid Rocket Company  
P. O. Box 13222  
Sacramento, Calif. 95813  
Attn: Dr. Sandy D. Rosenberg 1
  
35. Aerospace Corp.  
PO Box 92957  
Los Angeles, CA 90009  
Attn: Dr. Walter R. Warren, Jr. 1

36. Mr. A. Colin Stancliffe  
AIResearch Manuf. Co.  
2525 West 190th St.  
Torrance, CA 90503  
Attn: Dept. 93-6 1
37. Astro Research Corp.  
1330 Cacique  
Box 4128  
Santa Barbara, Calif. 93103  
Attn: R. F. Crawford, Dir. of Eng. 1
38. Atlantic Res. Corp.  
Shirley Highway at Edsall Rd.  
Alexandria, VA 22314  
Attn: Mr. Robert Naismith 1
39. AVCO - Everett Res. Lab.  
2385 Revere Beach Parkway  
Everett, MA 02149  
Attn: Dr. George Sutton 1  
Dr. Phillip Chapman 1
40. Battelle Columbus Laboratories  
505 King Ave.  
Columbus, O 43201  
Attn: Mr. Fred Tietzel (STOIAIC) 1
41. Bell Aerospace Co.  
Buffalo, N.Y. 14240  
Attn: Dr. Wayne C. Solomon 1

42. Boeing Co.  
PO Box 3999  
Seattle, WA 98124  
Attn: Mr. M. I. Gamble 1
43. ESL Inc.  
495 Java Dr.  
Sunnyvale, CA 94086  
Attn: Arthur Einhorn 1
44. Electro-Optical Systems  
300 N. Halstead  
Pasadena, CA 91107  
Attn: Dr. Andrew Jensen 1
45. General Electric Co.  
PO Box 8555  
Philadelphia, PA 19101  
Attn: Mr. W. J. East 1  
Dr. C. E. Anderson 1  
Dr. R. R. Sigismonti 1  
Dr. Thomas W. Karras 1
46. General Research Corp.  
PO Box 3587  
Santa Barbara, CA 93105  
Attn: Dr. R. Holbrook 1
47. Electro-Physics Laboratory 1  
University of Illinois  
Urbana, Ill. 61801  
Attn: Dr. T.A. Detemple

48. Hercules, Inc.  
PO Box 210  
Cumberland, MD 21502  
Attn: Dr. Ralph F. Preckel 1
49. Hughes Research Labs.  
3011 Malibu Canyon Rd.  
Malibu, CA 90265  
Attn: Dr. Arthur N. Chester 1  
Dr. Viktor Evtuhov 1
50. Hughes Aircraft Co.  
Centinela and Teale Sts.  
Culver City, CA 90230  
Attn: Dr. Eugene Peressini (Bldg. 6, MS/E-125) 1
51. Hughes Aircraft Co.  
PO Box 3310  
Fullerton, CA 90230  
Attn: Dr. William Yates 1
52. Institute for Defense Analyses  
400 Army Navy Dr.  
Arlington, VA 22202  
Attn: Dr. Alvin Schnitzler 1
53. Itek Corp.  
Optical Systems Div.  
10 Maguire Road  
Lexington, Mass. 02173  
Attn: R. J. Wollensak 1

54. Johns Hopkins University  
Applied Physics Lab.  
8621 Ga. Ave.  
Silver Spring, MD 20910  
Attn: Dr. Albert H. Stone 1
55. Lawrence Livermore Lab.  
PO Box 808  
Livermore, CA 94550  
Attn: Dr. R. E. Kidder 1  
Dr. E. Teller 1  
Dr. John Emmett 1
56. Los Alamos Scientific Labs.  
PO Box 1663  
Los Alamos, NM 87544  
Attn: Dr. Keith Boyer (MS 530) 1
57. Lulejian and Associates, Inc.  
Del Amo Financial Center Suite 500  
21515 Hawthorne Blvd  
Torrance, CA 90503 1
58. Lockheed Palo Alto Res. Lab.  
3251 Hanover St.  
Palo Alto, CA 94304  
Attn: L. R. Lunsford 1  
Orgn. 52-24, Bldg. 201
59. Mathematical Sciences Northwest, Inc.  
P. O. Box 1887  
Bellevue, WA 98009  
Attn: Mr. Abraham Hertzberg 1

60. Martin Marietta Aerospace  
PO Box 179  
Denver, COL 80201  
Attn: Mr. Stewart Chapin (Mail No. 0485) 1
61. Massachusetts Inst. of Technology  
Lincoln Lab.  
PO Box 73  
Lexington, MA 02173  
Attn: Dr. S. Edelberg 1  
Dr. R. H. Rediker 1
62. McDonnell Douglas Astronautics Co.  
5301 Bolsa Ave.  
Huntington Beach, CA 92647  
Attn: Mr. P. L. Klevatt 1  
Dept. A3-360-B3G0, M/S 14-1
63. McDonnell Douglas Res. Labs.  
Dept. 220, Box 516  
St. Louis, MO 63166  
Attn: Dr. D. P. Ames 1
64. MITRE Corp.  
PO Box 208  
Bedford, MA 01730  
Attn: Mr. A. C. Cron 1
65. Northrop Corporation  
Research & Technology Center  
3401 West Broadway  
Hawthorne, CA 90250  
Attn: Dr. M. M. Mann 1



66. Physical Sciences Inc.  
30 Commerce Way  
Woburn, Mass. 01801  
Attn: Dr. Anthony N. Pirri 1
67. Perkin Elmer Corp.  
Norwalk, Conn. 06852  
Attn: Dr. D. A. Dooley 1
68. Phaser Telepropulsion Inc.  
1888 Century Park East  
Suite 1606  
Los Angeles, Calif. 90067  
Attn: Dr. M. A. Minovitch 1
69. Radio Corporation of America  
Missile and Surface Radar Div.  
Morrestown, NJ 08057  
Attn: Mr. J. J. Mayman, Systems Project 1
70. RAND Corp.  
1700 Main St.  
Santa Monica, CA 90406  
Attn: Dr. Claude R. Culp 1
71. Razor Associates  
420 Persian Drive  
Sunnyvale, Calif. 94086  
Attn: Dr. Ned S. Razor 1

72. Raytheon Co.  
28 Seyon St.  
Waltham, MA 02154  
Attn: Dr. Frank A. Horrigan (Res. Div.) 1
73. Raytheon Co.  
Bedford Laboratories  
Missile Systems Div.  
Bedford, MA 01730  
Attn: Dr. H. A. Mehlhorn 1  
Optical Systems Dept.  
M/S S4-55
74. Riverside Research Institute  
80 West End St.  
New York, NY 10023  
Attn: Dr. L. H. O'Neill 1
75. R&D Associates, Inc.  
PO Box 3580  
Santa Monica, CA 90431  
Attn: Dr. R. E. LeLevier 1
76. Rockwell International Corp.  
3370 Miraloma Ave.  
Anaheim, CA 92803  
Attn: Dr. J. Winocur (D/528. HA14) 1

77. Rockwell International Corp.  
Rocketdyne Div.  
6633 Canoga Ave.  
Canoga Park, CA 91304  
Attn: Mr. Marc T. Constantine 1  
Dr. Stan V. Gunn 1
78. SANDIA Labs.  
PO Box 5800  
Albuquerque, NM 87115  
Attn: Dr. E. H. Beckner - Org. 5200 1
79. W. J. Schafer Associates, Inc.  
Lakeside Office Park  
607 N. Avenue, Door 14  
Wakefield, MA 01880  
Attn: Francis W. French 1
80. Stanford Research Institute  
Menlo Park, CA 94025  
Attn: Dr. R. A. Armistead 1
81. Science Applications, Inc.  
PO Box 2351  
La Jolla, CA 92037  
Attn: Dr. John Asmus 1
82. Mr. Lawrence Peckham  
-Science Applications, Inc.  
1911 N. Ft. Myer Drive, Suite 1200  
Arlington, VA 22209 1

83. Science Applications, Inc.  
PO Box 328  
Ann Arbor, MI 48103  
Attn: Dr. R. E. Meredith 1
84. Dr. Michael M. Monsler  
Science Applications, Inc.  
6 Preston Court  
Bedford, MA 01730 1
85. Systems Consultants, Inc.  
1050 31st St., N.W.  
Washington, D.C. 20007  
Attn: Dr. Robert B. Keller 1
86. Systems, Science and Software  
PO Box 1620  
LaJolla, CA 92037  
Attn: Mr. Alan F. Klein 1
87. Thiokol Chemical Co.  
WASATCH DIV.  
PO Box 524  
Brigham City, UT 84302  
Attn: Mr. James E. Hansen 1
88. TRW Systems Group  
One Space Park  
Bldg. 01, RM 1050  
Redondo Beach, CA 90278  
Attn: Mr. Norman F. Campbell 1

89. United Aircraft Res. Lab.  
400 Main St.  
East Hartford, CONN 06108  
Attn: Mr. G. H. McLafferty 1
90. United Aircraft Corp.  
Pratt and Whitney Div.  
Florida R&D Center  
West Palm Beach, FL 33402  
Attn: Dr. R. A. Schmidtke 1  
Mr. Ed Pinsley 1
91. VARIAN Associates  
EIMAC Div.  
301 Industrial Way  
San Carlos, CA 94070  
Attn: Mr. Jack Quinn 1
92. Vought Systems Div.  
LTV Aerospace Corp.  
PO Box 5907  
Dallas, TX 75222  
Attn: Mr. F. G. Simpson 1  
Mail Station 2-54142
93. Westinghouse Electric Corp.  
Defense and Space Center  
Friendship International Airport - Box 746  
Baltimore, MD 21203  
Attn: Mr. W. F. List 1
94. Westinghouse Res. Lab.  
Beulah Rd., Churchill Boro.  
Pittsburgh, PA 15235  
Attn: Mr. R. L. Hundstad 1